Reprinted from:

PROGRESS IN OPTICS

VOLUME V

EDITED BY

E. WOLF

University of Rochester, New York, U.S.A.

OPTICAL PUMPING

by

CLAUDE COHEN-TANNOUDJI AND ALFRED KASTLER

Laboratoire de Physique, Ecole Normale Supérieure, Paris 5e, France

1966

NORTH-HOLLAND PUBLISHING COMPANY-AMSTERDAM

I

OPTICAL PUMPING

BY

CLAUDE COHEN-TANNOUDJI AND ALFRED KASTLER
Laboratoire de Physique, Ecole Normale Supérieure, Paris 5e, France

CONTENTS

§ 1. Introduction

Optical pumping is a method for producing important changes in the population distribution of atoms and ions among their energy states by optical irradiation. The method of 'optical pumping' was proposed by one of the present authors in 1950 (KASTLER [1950]) as a method to change the relative populations of Zeeman levels and of hyperfine levels of the ground state of atoms. These population changes can be monitored by the change of intensity of the light transmitted by the sample in which optical pumping is produced or by the change of intensity or of polarization of the scattered resonance light. Population changes produced by thermal relaxation or by radiofrequency resonance can be detected in this manner.

The methods of optical pumping and of optical detection can also be used, either together or separately to investigate excited states of atoms. The pioneering work in this direction is the study of radiofrequency resonance in the excited state 6^3P_1 of the mercury atom, made by BROSSEL and BITTER [1952]. In this case polarized optical resonance radiation 2537 Å is used to obtain a selective excitation of Zeeman sublevels of the excited state, and magnetic resonance is detected by the change of polarization of the reemitted resonance radiation.

This method of studying excited states was called the 'double-resonance' method by its authors. Two resonances, an optical resonance and a magnetic resonance are associated in it. More generally, two monochromatic radiations of different frequencies in the electromagnetic spectrum are simultaneously applied to an atomic system. Since 1950, both excited states and ground states of atoms have been studied extensively by optical pumping and by optical detection methods. An excellent review on the results obtained on excited states has been published by SERIES [1959].

In the present paper we restrict ourselves to review the results ob-

tained on ground states or on metastable atomic states, taking the word 'optical pumping' in the restrictive sense first used (KASTLER [1950]) which implies a two-step process (Fig. 1):

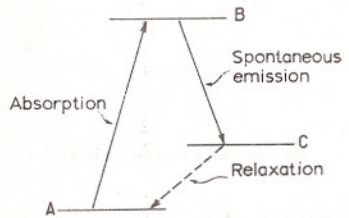

Fig. 1. Optical-pumping scheme.

The first step AB is an upward process of induced absorption of light — which is space-directed and polarized and in some cases also frequency-selected — producing absorption starting from an initial A-state, the second step BC is a spontaneous downward process consisting either in spontaneous emission of light or in a rapid radiationless relaxation process.

In this manner, the population ratio of levels A and C is changed, the population of A level being decreased and the population of C level being enhanced. The amount of change obtained in a stationary process depends on the intensity of the pumping light applied to the atoms and on the velocity of the relaxation processes which tend to restore thermal equilibrium among the A- and C-state populations.

The C state may be an electronic level distinct from the A state, or A and C may be two magnetic or hyperfine sublevels of the same electronic state which is in general the ground state or a metastable long-living state. The method of optical pumping keeps its efficiency even in the case where these sublevels A and C are degenerate.

If in the energy scale the C state is located above the A state, the energy of the atomic system is enhanced in the two-step pumping process. In this case optical pumping is a 'heating' process. If A and C are the two magnetic sublevels of a spin state $\frac{1}{2}$, the 'spin temperature' of the system is raised by optical pumping.

If a population inversion between C and A is reached, the system is placed in a state of 'negative absolute temperature.'

If in the energy scale the C state is located below the A state, optical pumping is a 'cooling' process. The spin temperature of the system is lowered.

In the case of Zeeman levels in a magnetic field, the change from heating to cooling can be easily achieved either by reversal of the applied magnetic field or by reversal of the circular polarization of the pumping light.

The change of population produced by optical pumping is associated not only with a change of energy of the atomic assembly, but also with a peculiar change of angular momentum. Angular momentum is transferred from the light to the assembly of atoms †. To each atomic quantum state belongs a given energy, and also a definite spin vector and magnetic momentum vector, these vectors being defined in magnitude and in quantized orientation in space. By optical pumping, polarization (and alignment) of the spin vectors is produced, and macroscopic magnetization of the medium is obtained.

Optical pumping has been reviewed already at different occasions (KASTLER [1954, 1957a, b, 1960, 1962, 1963a], BROSSEL [1957, 1960a, b, c, 1961], SKROTSKY [1961], SKALINSKI [1960], BITTER [1962], BLOOM [1960b], ZAFRA [1960], CARVER [1963], BENUMOF [1965]).

The four last mentioned papers are written in a popular way suitable for non-specialists.

§ 2. Principles of Optical Pumping

2.1. PRODUCTION OF ATOMIC OR NUCLEAR ORIENTATION

2.1.1. *Different pumping procedures*

2.1.1.1. Zeeman pumping in pure vapours

Such pumping produces unequal populations of different magnetic sublevels of the ground state of atoms. Let us take an example: the case of an alkali atom in its ground state which is a $^2S_{\frac{1}{2}}$ state with electron spin $\frac{1}{2}$ divided by a magnetic field into two Zeeman sublevels: $m = -\frac{1}{2}$ and $m = +\frac{1}{2}$. For simplicity let us disregard nuclear spin. (An alkali-atom configuration without nuclear spin is realized in the $^{40}Ca^+$ ion.) By absorption of optical resonance radiation (the D_1 and D_2 lines of sodium), the atom is raised to the $^2P_{\frac{1}{2}}$ and $^2P_{\frac{3}{2}}$ states which are the excited states nearest to the ground state.

Figures 2a, b show the Zeeman structure of the levels involved and of the spectral transitions between them: Figure 2a is an energy scheme:

† The principle of conservation of angular momentum in the interaction of light and matter was introduced in atomic physics in the early days of the old quantum theory by A. RUBINOWICZ [1918].

the energy of the state is given by the vertical position of the horizontal line representing the state. Spectral transitions are indicated by

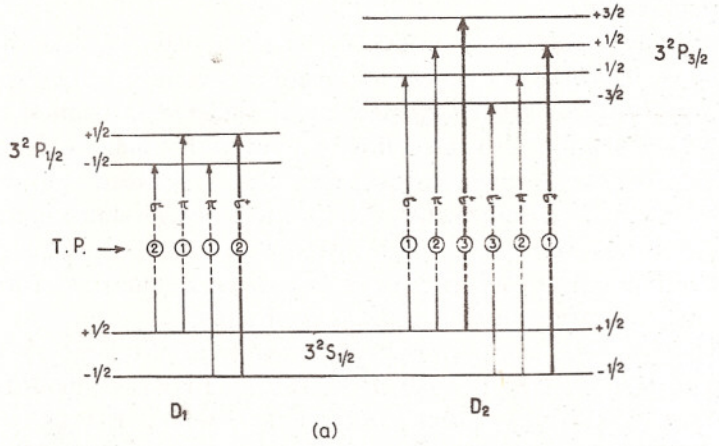

Fig. 2a. Zeeman structure of the D_1 and D_2 resonance lines of alkali atoms. Energy scheme. T.P. = Transition Probabilities.

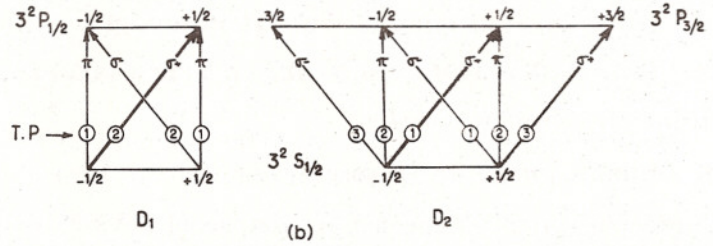

Fig. 2b. Zeeman structure of the D_1 and D_2 lines. Polarization scheme.

vertical arrows. Figure 2b is a polarization scheme: magnetic sublevels of a same state are represented by equidistant points on a horizontal line. The arrows indicate the Zeeman transitions.

In this scheme vertical arrows correspond to $\Delta m = 0$ or π transitions, arrows with a positive slope to $\Delta m = +1$ or σ^+ transitions, arrows with a negative slope to $\Delta m = -1$ or σ^- transitions.

The circled numbers (T.P.) indicate the relative transition probabilities in an arbitrary scale.

We recall the selection rules for Zeeman lines of a dipole transition: only $\Delta m = 0$ and $\Delta m = \pm 1$ transitions are allowed. The polarization rules for electric dipole transitions are the following:

$\Delta m = m' - m''$ (m' = magnetic quantum number of the upper state
m'' = magnetic quantum number of the lower state).

$\Delta m = 0$ corresponds to π polarization: the light is linearly polarized with its electric vector parallel to the magnetic field, $\Delta m = +1$ corresponds to σ^+ polarization: the light is circularly polarized in a plane perpendicular to the field. The sense of rotation is the sense of the electric current in a coil generating the magnetic field. $\Delta m = -1$ corresponds to σ^- polarization: the light is circularly polarized in a plane perpendicular to the field. The sense of rotation is opposite to σ^+. For magnetic dipole transitions the selection rules are the same. In the polarization rule the word 'electric vector' has to be replaced by 'magnetic vector' of the electromagnetic radiation field.

An observer looking in the field direction and receiving light propagated in the direction opposite to the field sees σ^+ light rotating clockwise and calls it 'right-handed polarized'.

An observer looking in the opposite direction and receiving light propagated in the field direction sees σ^+ light rotating anti-clockwise and calls it 'left-handed polarized'.

The atoms are illuminated with circularly polarized resonance radiation, say σ^+. Suppose that the incident light contains only the D_1 line. In this case, only one of the upward transitions shown in Fig. 2 will take place. Atoms from the $m = -\frac{1}{2}$ level of the ground state will be raised to the $m = +\frac{1}{2}$ level of the upper state. Falling back by spontaneous emission to the ground state, part of them will return to the initial Zeeman level, part of them will transit – by emission of the π component – to the $m = +\frac{1}{2}$ level of the ground state. According to the transition probabilities from three atoms having each absorbed one photon, two will return to the initial level and one will go to the $+\frac{1}{2}$ level.

From one hundred atoms, half of them are initially in the $m = -\frac{1}{2}$ level and half of them in the $m = +\frac{1}{2}$ level of the ground state. If each of the fifty atoms which are able to absorb circularly polarized photons has absorbed one photon, $\frac{50}{3}$ atoms will have been pumped from the $-\frac{1}{2}$ to the $+\frac{1}{2}$ level. The populations will then be

$$N_{+\frac{1}{2}} = 50 + \tfrac{50}{3} = 100 \times \tfrac{2}{3} \qquad \text{for the } +\tfrac{1}{2} \text{ level.}$$
$$N_{-\frac{1}{2}} = 50 - \tfrac{50}{3} = 100 \times \tfrac{1}{3} \qquad \text{for the } -\tfrac{1}{2} \text{ level.}$$

There will be twice as many atoms in one level than in the other one. The degree of polarization, defined by

$$P = \frac{N_{+\frac{1}{2}} - N_{-\frac{1}{2}}}{N_{+\frac{1}{2}} + N_{-\frac{1}{2}}} = \tfrac{1}{3}$$ will be 33 % in this case.

After a small number of absorption processes a high degree of population change can be obtained in this manner. If both D_1 and D_2 lines are used for optical pumping and are σ^+ polarized, the line $-\frac{1}{2} \rightarrow +\frac{1}{2}$ of D_2 will contribute to the pumping. Absorption of the line $+\frac{1}{2} \rightarrow +\frac{3}{2}$ of D_2 also takes place in this case, but it does not contribute to the pumping. This is unimportant as long as no perturbation occurs while the atoms are in the excited state. In many practical cases D_1 and D_2 are used together to achieve pumping.

2.1.1.2. Pumping in presence of a buffer-gas — (Dehmelt type pumping)

In the preceding description of the pumping process, we supposed that the atom pumped by the incoming light to the excited state, remains in a definite magnetic sublevel of this excited state before it falls back to the ground state. This is the case in dilute vapours where the mean free time between two collisions is much longer than the life-time of the excited state. The situation becomes different if we add a foreign gas to the vapour which is pumped. If the pressure of this gas is high enough, the mean free time for collisions becomes smaller than the life-time of the excited state and most of the excited atoms undergo collisions with foreign gas molecules before they return to the ground state. The effect of such collisions is to induce transfers between Zeeman levels (and hyperfine levels) of the excited state. As a result of these transfers the emitted optical resonance radiation is completely depolarized (MITCHELL–ZEMANSKY [1934] ch. V).

The question arises: Is optical pumping still efficient in this case to orient atoms in the ground state? If atoms undergo collisions with foreign gas molecules during their short stay in the excited state they also frequently undergo collisions in the ground state. Optical pumping can only remain efficient under these conditions if these ground-state collisions do not disorient the atoms, if they do not induce transitions between Zeeman levels of the ground state.

P. BENDER [1956] has shown that collisions do not induce transfers between magnetic sublevels of the electronic state in an S state. In this case, the magnetic moment is a pure spin moment. Transfers are induced if the electronic state of the atom is a P or D state, if part of the magnetic moment is orbital moment.

For most atoms on which optical pumping is made the ground state is an S state (alkali atoms, mercury, etc.), the excited state is a P state. This explains why these atoms are sensitive to collisions in their excited state sublevels, and why they are insensitive to collisions in the ground-state sublevels.

For oriented ground-state atoms diamagnetic foreign gases act as 'buffer gases'. Their collisions do not only preserve ground-state orientation but they also prevent atoms from going to the walls.

If the buffer-gas pressure is high enough optically excited atoms will be randomly distributed among the Zeeman levels of the excited state before they return to the ground state. As a result of this they will return at equal rate to all Zeeman levels of the ground state. In this extreme case the efficiency of pumping depends only on the rate by which the exciting light is absorbed from the different Zeeman levels of the ground state. Let us consider again the case of the D_1 and D_2 lines of an alkali atom. If we illuminate the atoms with σ^+ of both D_1 and D_2, and if these two lines have equal intensity, we see that the sum of transition probabilities of σ^+ components starting from each m level of the ground state is the same ($1+2$ for $m = -\frac{1}{2}$ and 3 for $m = +\frac{1}{2}$). Both m levels will be emptied at the same rate and filled up again at the same rate. In these conditions, optical pumping will be inefficient. But it becomes efficient if we suppress the D_2 light by a suitable filter and if we use only D_1 light for pumping.

We see immediately that in this case only $m = -\frac{1}{2}$ atoms will be excited, and pumping will result in a rarefaction of atoms in the $m = -\frac{1}{2}$ state and a concentration in the $m = +\frac{1}{2}$ state.

An alternative procedure would be to use both the D_1 and D_2 lines and to polarize them circularly in opposite sense, for example $D_1\,\sigma^+$ and $D_2\sigma^-$. The ratio of transition probabilities from $m = +\frac{1}{2}$ and $m = -\frac{1}{2}$ would be in this case 5 : 1 and a high degree of polarization could be achieved.

We see that optical pumping in vapours can be efficient without or with buffer gas, but that the optimum pumping conditions are not the same in both cases. Different illumination conditions have to be used to obtain in each case the best efficiency of pumping.

2.1.1.3. Hyperfine pumping

Optical pumping has been first used to concentrate atoms in given Zeeman sublevels of the ground state using circularly polarized light. It was soon realized that the production of strong population differences between hyperfine levels is also of interest and that it can be achieved by optical-pumping techniques.

In the case where the ground state has a hyperfine structure it can be shown – by analysing the scheme of the Zeeman structure of the different hyperfine components of the pumping light – that ordinary Zeeman pumping with circularly polarized light, but without selection of hyperfine components in the pumping light is always accompanied by a certain amount of hyperfine pumping.

For example, in the case of alkali atoms with nuclear spin $i = \frac{3}{2}$ (^{23}Na, ^{39}K, ^{87}Rb) where the ground state $S = \frac{1}{2}$ is split into two hyperfine levels $F = 2$ and $F = 1$, pumping with σ^+ light in pure vapour would – if all relaxation processes would be negligibly slow – concentrate all atoms in the $m_F = +2$ state of the $F = 2$ state. The $F = 1$ state would be totally emptied.

Hyperfine pumping can be more efficiently achieved by selection of hyperfine components in the pumping light. Hyperfine components of a spectral line are very close together and it is difficult to separate them by ordinary filter techniques. In some cases, nature fortunately provides us with selective light sources in the case where different isotopes of the same element are available. This is especially the case for rubidium and mercury.

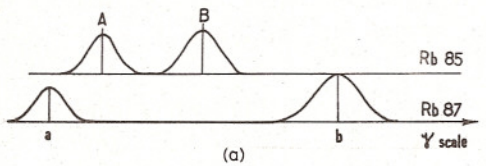

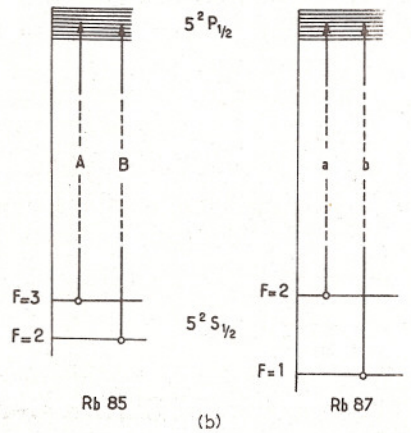

Fig. 3a. Hyperfine structure of the resonance line $D_1 (5^2S_{\frac{1}{2}} \rightarrow 5^2P_{\frac{1}{2}})$ of ^{85}Rb and ^{87}Rb in the frequency scale.

Fig. 3b. Energy scheme of the hyperfine structure of the D_1 line of Rb.

Figure 3a shows the hyperfine structure of the infrared resonance line 7947 Å of Rb ($5^2S_{\frac{1}{2}} \rightarrow 5^2P_{\frac{1}{2}}$) for the two isotopes ^{85}Rb (spin $i = \frac{5}{2}$) and ^{87}Rb (spin $i = \frac{3}{2}$).

As the hyperfine intervals of the excited state ($5^2P_{\frac{1}{2}}$) are much smaller than the intervals of the ground state ($5^2S_{\frac{1}{2}}$) the line of each isotope consists practically of two hyperfine components (A and B for ^{85}Rb and a and b for ^{87}Rb).

In the wave-number scale the distance of components AB is about 0.10 cm^{-1} and the distance of components ab is more than twice this value (0.23 cm^{-1}). The Figure shows the relative positions of the four components in the spectrum. Components A and a are nearly coincident and overlap by Doppler broadening, components B and b are completely separated. Figure 3b shows the energy scheme of the hyperfine structure of both isotopes. The situation is analogous for the line $5^2S_{\frac{1}{2}} \rightarrow 5^2P_{\frac{3}{2}}$ and also for the blue and ultraviolet absorption-lines starting from the ground state.

If a resonance cell containing ^{87}Rb is illuminated with the light of a lamp containing ^{85}Rb, component A of the lamp line will excite the *a* transition of the ^{87}Rb atoms in the resonance cell. In this case only the upper hyperfine level $F = 2$ of the ^{87}Rb atoms will be pumped by the incoming light. The population of the upper $F = 2$ level will decrease and the population of the lower $F = 1$ level will increase.

If a resonance cell containing ^{87}Rb is illuminated with a ^{87}Rb lamp whose light is filtered through a ^{85}Rb absorption cell (Fig. 4) the a component of the lamp will be removed by the filter, and the ^{87}Rb atoms of the resonance cell will be pumped only by the b component. In this case, the lower level $F = 1$ will be emptied and the upper

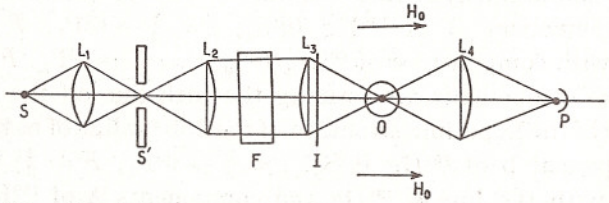

Fig. 4. Mounting for hyperfine pumping of ^{87}Rb by the b component.

S–^{87}Rb lamp
F–^{85}Rb filter
L_1, L_2, L_3, L_4 – Lenses
O–^{87}Rb resonance cell
P–Photo-detector
I–Interference filter

level $F = 2$ of the ground state will be filled up. Population inversion between these two levels can be obtained easily in this way. Attempts are made to start in this manner a maser operating on the $F = 2 \rightarrow F = 1$ transition of ^{87}Rb (6835 Mc/s)†.

Conversely ^{85}Rb atoms in a resonance cell can be pumped by the same procedure: With a ^{87}Rb lamp concentration in the lower $F = 2$ state will be obtained, with a ^{85}Rb lamp and a ^{87}Rb filter concentration in the upper $F = 3$ state will result.

These methods of hyperfine pumping are used in the optically pumped Rb-atomic frequency standards (§ 4.2).

The case of mercury is also interesting for selective hyperfine pumping. Figure 5 shows the hyperfine structure of the ultraviolet resonance line 2537 Å of mercury. It consists of five components, four of

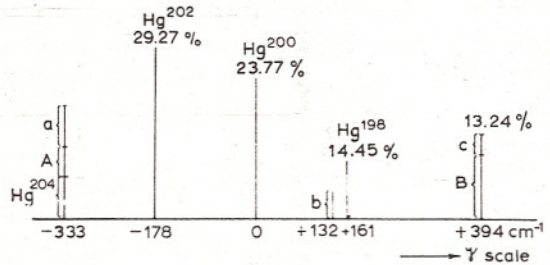

Fig. 5. Hyperfine structure of Hg 2537 Å, frequency scale.

them being the single lines of the even isotopes 204, 202, 200 and 198 present at a high concentration in natural mercury. Natural mercury contains two odd isotopes, ^{199}Hg at a concentration of 16 % and ^{201}Hg at a concentration of 13 %, their respective nuclear spins being $\frac{1}{2}$ and $\frac{3}{2}$. Figure 6 shows the hyperfine structure of 2537 Å for these two odd isotopes. Component B of ^{199}Hg (6^1S_0, $i = \frac{1}{2} \rightarrow 6^3P_1$, $F = \frac{3}{2}$), is coincident with component c of ^{201}Hg(6^1S_0, $i = \frac{3}{2} \rightarrow 6^3P_1$, $F = \frac{1}{2}$).

These two components are forming the fifth line on the high-frequency side of the hyperfine structure of the 2537 Å line of natural mercury. Component b of ^{201}Hg (6^1S_0, $i = \frac{3}{2} \rightarrow 6^3P_1$, $F = \frac{3}{2}$) is nearly coincident with the line of ^{198}Hg and components A of ^{199}Hg (6^1S_0, $i = \frac{1}{2} \rightarrow 6^3P_1$, $F = \frac{1}{2}$) and a of ^{201}Hg(6^1S_0, $i = \frac{3}{2} \rightarrow 6^3P_1$, $F = \frac{5}{2}$) are nearly coincident with the line of ^{204}Hg. By 'nearly coincident' we mean that the line centers are not exactly coincident, but that the

† Self-sustained maser oscillations on an optically pumped ^{87}Rb cell have been obtained recently: DOVIDOVITS and STERN [1965], ARDITI and CARVER [1965].

lines are overlapping because of Doppler broadening; the distance of the line centers being smaller than 0.05 cm^{-1}.

Working on ^{199}Hg in a resonance cell, we are able to excite its component A separately (without exciting component B) by illuminating the cell with a ^{204}Hg lamp.

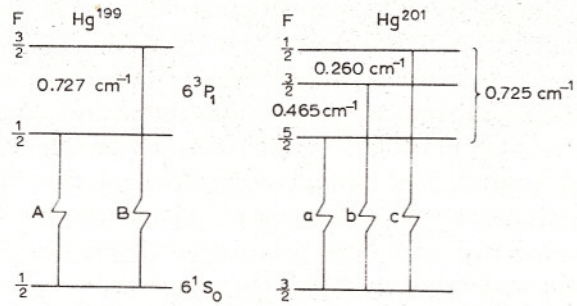

Fig. 6. Energy scheme of the hyperfine structure of Hg 2537 Å for the odd isotopes ^{199}Hg ($i = \frac{1}{2}$) and ^{201}Hg ($i = \frac{3}{2}$).

Working on ^{201}Hg, we can either excite only component a with a ^{204}Hg lamp or we can excite only component b with a ^{198}Hg lamp.

These examples show the usefulness of having available separated isotopes. For optical-pumping techniques very small quantities are needed (1 mg for a resonance cell, 5 or 6 mg for a long-living electrodeless lamp), but a high enrichment factor (99 %) is desirable.

Analogous techniques of hyperfine pumping can be used for the

TABLE 1

Hyperfine structure of Hg 2537 Å and of Hg 1850 Å

For each line the component of ^{198}Hg is taken at zero position. The distances to this line are given in $10^{-3} \cdot$ cm^{-1}.

Isotope component	F level of the excited state	2537 Å	1850 Å
198		0	0
199 A	$\frac{1}{2}$	−514	+96
199 B	$\frac{3}{2}$	+224.4	−79.8
200		−160.3	−156
201 c	$\frac{1}{2}$	+229.3	−318
201 b	$\frac{3}{2}$	− 22.6	−256
201 a	$\frac{5}{2}$	−489.0	−149
202		−337.0	−329
204		−510.8	−519

mercury resonance line 1850 Å ($6^1S_0 \rightarrow 6^1P_1$), whose hyperfine structure is different † and given in Table 1.

In the many cases where nature does not provide us with natural coincidences of lines, magnetic and electric scanning techniques are useful to achieve artificial coincidences by Zeeman or by Stark displacements (BITTER [1962], BEATY *et al.* [1958]).

Magnetic scanning techniques are of special interest in the far ultraviolet where light polarizing devices are not available. By Zeeman splitting linearly or circularly polarized Zeeman-components can be produced and brought into coincidence with absorption lines. Pumping with π or σ light or with σ^+ or σ^- light can thus directly be achieved (OMONT and BROSSEL [1961]). For example, using the mercury line 1850 Å for pumping, atoms of isotope 201 can be pumped on the component ($i = \frac{3}{2} \rightarrow F = \frac{1}{2}$) with circularly polarized σ^+ light, by using a light source of ^{202}Hg in a longitudinal magnetic field of 500 to 600 gauss. A strong nuclear polarization can be obtained in this manner. It can be reversed by reversal of the magnetic field applied to the light source.

2.1.1.4. Selection of fine structure components

In § 2.1.1.3, we have seen that the use of different isotopes in the resonance cell and in the exciting light source gives the possibility of selective pumping on hyperfine components. The same technique can

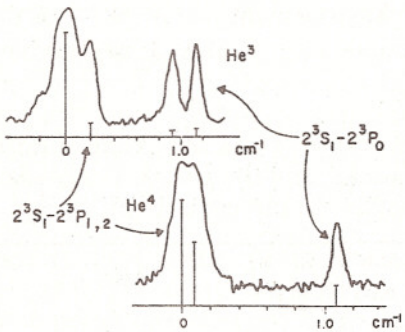

Fig. 7. Structure and isotope shift for the 2^3S–2^3P spectral line of helium (10 830 Å). After FRED *et al.* [1951].

be used for selective pumping of fine-structure components for the light elements where fine structure components are close together. This

† Interesting work on this line has been started by Popescu and Novikov [1964] at the Laboratory of the Ecole Normale Supérieure de Paris.

type of pumping has been used on ^{3}He to pump the fine-structure component $2^3S_1 \rightarrow 2^3P_0$ of the 1.083 micron-line by using a ^{4}He lamp. Figure 7 shows that the fine structure component $2^3S_1 \rightarrow 2^3P_{1,2}$ of ^{4}He is coincident with the fine-structure component $2^3S_1 \rightarrow 2^3P_0$ of ^{3}He.

This selective pumping of ^{3}He in the metastable 2^3S_1 state has been successfully used, combined with circular polarization to obtain a high degree of nuclear polarization in the 2^3S_1 state of a ^{3}He gas (COLEGROVE *et al.* [1963]).

2.1.1.5. Pumping with exchange collisions

If a vapour is a mixture of two paramagnetic species, for example rubidium and cesium, the experiment shows that if the atoms of one species are oriented by optical pumping, the orientation is transferred to the atoms of the other species. This transfer of orientation occurs through exchange collisions: During these collisions the valence electrons of the two colliding atoms are exchanged, each electron keeping its spin orientation. Symbolically we may write the exchange reaction:

$$A\uparrow + B\downarrow \rightarrow A\downarrow + B\uparrow$$

where the arrows indicate the orientation of the spin vectors of the valence electrons.

The following species have been oriented by mixing them with optically pumped alkali vapours:

^{1}H, ^{2}H, ^{3}H, ^{14}N, ^{15}N, ^{32}P and free electrons.

Exchange collisions can occur also between two isotopes of the same element, e.g. between ^{87}Rb and ^{85}Rb.

During exchange collisions, nuclear orientation is preserved to a certain extent. A special case of exchange collisions is the 'metastability exchange' which corresponds to a very large cross section and which occurs when a ground-state atom and a metastable atom collide with each other. The energy of the metastable atom is transferred to the colliding atom. It is impossible to detect such a transfer if the two atoms have zero nuclear spin, because they are undistinguishable then. This is the case for ^{4}He.

But if a nuclear moment is present (^{3}He, $i = \frac{1}{2}$) and if the nucleus in the metastable state has been polarized ($m_i = +\frac{1}{2}$), the nuclear orientation – in the metastability-exchange process – becomes nuclear orientation of a ground-state atom.

In this manner nuclear orientation obtained on metastable atoms (2^3S_1 atoms of ^3He) can be transferred to ground-state atoms at a rapid rate (COLEGROVE *et al.* [1963]).

2.1.2. *Conditions to be fulfilled for efficient pumping*

By optical pumping high degrees of atomic polarization or of nuclear polarization can be obtained, but the pumping process is always counteracted by the thermal relaxation processes which tend to restore thermal equilibrium among the spins. In given experimental conditions one relaxation process is in general dominant and can be characterized by a definite relaxation time T_1. If the optical-pumping light is suddenly interrupted by a shutter, the macroscopic magnetic moment $\langle M_z \rangle$ induced in the vapour by the pumping process will decay exponentially, according to the law

$$M_z(t) = M_z(0)\exp(-t/T_1).$$

Let us consider the simple case where the ground state of an atom is an $S = \frac{1}{2}$ state having only two magnetic sublevels $m = -\frac{1}{2}$ and $m = +\frac{1}{2}$. If μ is the magnetic moment of a ground-state atom and if N_+ and N_- are the respective numbers of atoms in the states $+\frac{1}{2}$ and $-\frac{1}{2}$, the magnetic moment of the assembly of atoms is given by

$$\langle M_z \rangle = \mu(N_+ - N_-).$$

The degree of polarization P can be defined by

$$P = \frac{N_+ - N_-}{N_+ + N_-} = \frac{N_+ - N_-}{N} = \frac{\langle M_z \rangle}{\mu N}$$

where N is the total number of atoms which is constant.

P and $\langle M_z \rangle$ are two quantities which are proportional to each other. Let us denote by $n = N_+ - N_-$ the difference of populations between $m = +\frac{1}{2}$ and $m = -\frac{1}{2}$.

The decay law which we have mentioned results from the differential equation

$$dn/dt = -n/T_1$$

which governs the relaxation process.

Obviously this relaxation process, which is present in the dark, is also present during light illumination.

By the action of light, atoms are pumped from the $m = -\frac{1}{2}$ level to the $m = +\frac{1}{2}$ level of the ground state at a rate which is proportional to the incoming light intensity $\mathcal{I}$ and to the number of atoms N_- remaining in the $-\frac{1}{2}$ level. The differential equation of pumping will be

$$dN_+ = -dN_- = K\mathcal{I}N_- dt,$$

which can be written as

$$dn = d(N_+ - N_-) = 2K\mathcal{I}[\tfrac{1}{2}(N-n)dt]$$

if we note that $N_- = \frac{1}{2}(N-n)$.

Introducing a 'pumping time' T_P by $1/T_P = K\mathcal{I}$ the pumping equation takes the form

$$\frac{dn}{dt} = \frac{N-n}{T_P}.$$

The total change of n when pumping and relaxation are simultaneously acting is

$$\frac{dn}{dt} = \frac{N-n}{T_P} - \frac{n}{T_1}$$

If a steady state is reached, dn/dt must be zero.

The steady-state polarization corresponds to

$$n_0 = N(1+T_P/T_1)^{-1}$$

and

$$\langle M^0{}_z \rangle = \mu n_0.$$

To obtain a strong steady-state polarization ($n_0 \geqq \frac{1}{2}N$) we must satisfy the condition $T_P \leqq T_1$. The pumping rate must be higher than the relaxation rate.

For a good pumping rate a high efficiency of the light source is needed. With ordinary commercial spectral lamps, pumping times of the order of 10^{-4} s can be obtained.

The most efficient light sources are small electrodeless lamps which are high-frequency excited. To avoid self-reversal of the resonance lines, a small thickness of the emitting layer (1 mm for mercury lamps, 4 or 5 mm for alkali-vapour lamps) is favourable. Figure 8 shows the size and the shape of such a lamp for Rb vapour: the lamp is made with two parallel plane glass-windows and has a reservoir. It must be thoroughly baked out in vacuum before filling it with a small quantity of metal and a noble gas (argon) at about 1 mm pressure.

Because the quantity of metal that is needed is very small (5 mg), this type of lamp is very convenient when using pure isotopes. Such

lamps can operate for hundreds of hours and have a high efficiency for exciting resonance radiation of atoms. The breadth of the emission lines is only about the Doppler breadth at ordinary temperature.

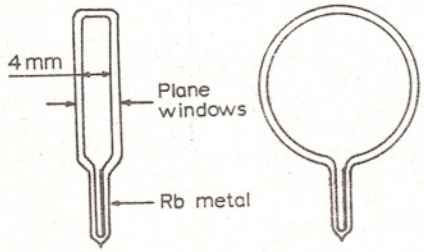

Fig. 8. Electrodeless lamp for alkali metals.

In order to obtain a strong steady state polarization, it is also useful to make the relaxation as slow as possible. The first optical-pumping experiments have been made on atomic beams where relaxation is absent but where the time of pumping is limited to the time of flight of the atoms across the light beam.

For a beam of atoms illuminated along a path of 20 cm, with a mean thermal velocity of 500 m/s, this time is of the order of 4×10^{-4} s. This is sufficiently long to obtain a high degree of polarization. But it is experimentally simpler and easier to work on diluted vapours in a sealed bulb. For an alkali vapour in a glass bulb each wall collision disorients completely the atoms. The relaxation time is the mean time of flight between two wall collisions. This time is of the order of 10^{-4} s. The relaxation rate can be considerably slowed down either by covering the glass wall of the bulb with special coatings (paraffines or silicones) or by adding to the vapour a buffer gas, or by using both the coating and the buffer gas. We will study these methods in detail in § 3.3.

2.1.3. *The aim of optical pumping*

Optical pumping is a powerful method to create and to maintain a non-equilibrium situation of populations of atoms in different quantum states.

These states can be states of different energy, different fine-structure levels (J), different hyperfine-structure levels (F) or different Zeeman sublevels (m_J, m_F, m_i). In the latter case we achieve atomic or nuclear orientation. This orientation is called 'polarization' if a population difference is produced between positive and negative m levels.

The degree of polarization may be defined by

$$P = \frac{1}{J}\frac{\sum_m mN_m}{\sum_m N_m}.$$

Complete polarization corresponds to $P = +1$ or $P = -1$.

Polarization is accompanied by a macroscopic magnetization of the paramagnetic vapour:

$$\langle M_z\rangle = N\mu P = \frac{\mu}{J}\sum_m mN_m.$$

Polarization is obtained by pumping with circularly polarized σ^+ or σ^- light. In certain circumstances, if the vapour is in a suitable magnetic field, polarization effects can be obtained with natural unpolarized σ light.

The orientation is called 'alignment' if a population difference is produced between states of different $|m|$. An example of such alignment is obtained when mercury vapour of ^{201}Hg ($i = \frac{3}{2}$) is illuminated with natural (but unidirectional) σ light of a frequency corresponding to the hyperfine component c ($i = \frac{3}{2} \to F = \frac{1}{2}$).

Figure 9 shows that in this case levels $m = \pm\frac{3}{2}$ are three times more rapidly pumped than levels $m = \pm\frac{1}{2}$, so that the population of $\pm\frac{3}{2}$ will decrease and the population of $\pm\frac{1}{2}$ will increase. The population difference is inverted if we use π light for pumping instead of σ light.

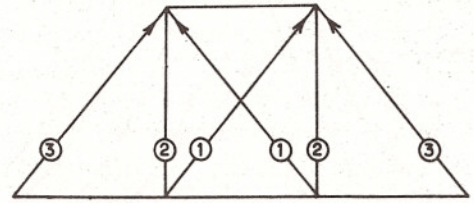

Fig. 9. Zeeman structure of the c hyperfine component ($i = \frac{3}{2} \to F = \frac{1}{2}$) of 2537 Å of ^{201}Hg.

The question now arises: Once atoms or nuclei are oriented, what can we do with them?

Oriented nuclei may be used for specific experiments in nuclear physics. Oriented radioactive nuclei will show anisotropy of γ radiation or dissymmetry of β emission (SIBILLA [1962]).

Non-radioactive oriented nuclei can be used as oriented targets or as a source for oriented ion beams (e.g., oriented ^{3}He^{++} ions).

Optically oriented atoms enable us to study the relaxation processes by which they return to thermal equilibrium. We shall return to this problem later on.

The most important application of optically pumped atoms or nuclei is the investigation of radiofrequency resonance transitions: Ordinary Zeeman transitions $\Delta F = 0$, $\Delta m_F = \pm 1$ and hyperfine transitions $\Delta F = 1$, $\Delta m_F = 0$ or ± 1 can be studied in this way. By optical pumping large population differences between F, m_F levels are obtained. If a radiofrequency magnetic field is applied on resonance with a transition F', $m'_F \rightleftarrows F''$, m''_F the populations of these two magnetic sublevels are equalized and a strong light signal results. Figure 10 shows magnetic-resonance curves obtained by CAGNAC [1960] on the nuclear transition $m_i = -\frac{1}{2} \rightleftarrows +\frac{1}{2}$ in the ground state 6^1S_0 of ^{199}Hg. Each curve corresponds to a given amplitude H_1 of the radiofrequency field.

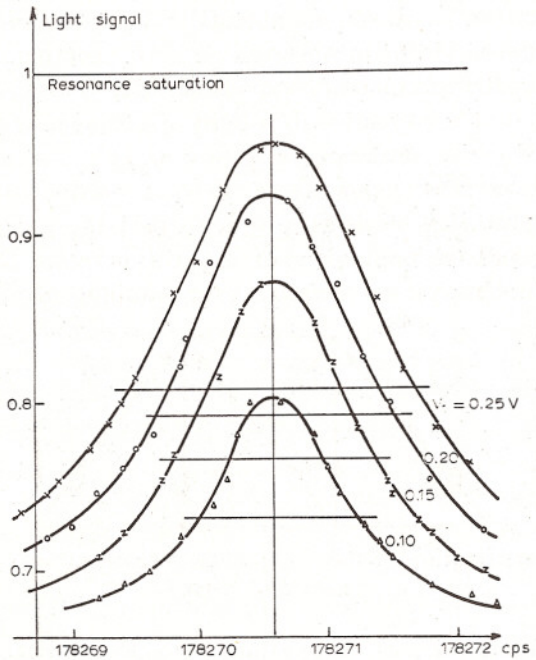

Fig. 10. Nuclear magnetic resonance curves of the ground state of ^{199}Hg (CAGNAC [1960]), frequency scale.

The curves show the usual radiofrequency broadening effect (the width at half-maximum is indicated for each curve). An extrapolation to zero r.f.-amplitude leads to a width $\Delta\omega = 1/\tau_2$ of the line in the ω scale.

$\Delta\omega$ is still a function of the pumping-light intensity $\mathcal{I}$. A second extrapolation to zero-light intensity leads to the intrinsic width

$$\Delta\omega_0 = 1/T_2,$$

where T_2 represents the transverse relaxation time due to thermal relaxation which can be determined in this manner.

The study of radiofrequency-resonance signals by optical-pumping techniques has lead to interesting new results:

Previously unknown hyperfine intervals in the ground state of atoms (^{14}N, ^{15}N, ^{31}P) have been measured (ANDERSON and PIPKIN [1959], HOLLOWAY *et al.* [1962], LAMBERT and PIPKIN [1962, 1963]), spin-resonance of free electrons has been demonstrated (DEHMELT [1958], HOBART [1962], BALLING *et al.* [1964]), multiple quantum transitions have been discovered (BROSSEL *et al.* [1953], MARGERIE and BROSSEL [1955], MARGERIE *et al.* [1955]) and systematically investigated (WINTER [1955a, b, 1959], SALWEN [1955, 1956], HACK [1956]).

New quantum effects: displacements of energy levels of atoms by real and by virtual optical transitions have been theoretically predicted (BARRAT and COHEN-TANNOUDJI [1961]) and experimentally confirmed (COHEN-TANNOUDJI [1962a]).

2.2. OPTICAL DETECTION OF ATOMIC ORIENTATION

Atomic orientation is achieved by light in the optical-pumping process. The population changes produced by this pumping can be monitored by an optical light signal. Different methods of detection can be used: measurement of the intensity of the direct pumping beam transmitted by the vapour, measurement of the intensity or of the polarization of the resonance or fluorescence light scattered at right angle of the incident beam, modification of a secondary light beam – distinct from the primary beam – transmitted by the vapour.

We will now review those three methods:

2.2.1. *Measurement of the intensity of the direct light beam transmitted by the absorbing vapour*

This method is based on the fact that the absorption coefficient of an oriented vapour for light is different from the absorption coefficient of the vapour in a disoriented state. Let us consider two spectral lines, one of type D_1, the other of type D_2, both being pumped with cir-

cularly polarized σ^+ light (Fig. 2). Only atoms in the $m = -\frac{1}{2}$ state are able to absorb circularly polarized D_1 light.

If, as a result of pumping, N_- decreases and N_+ increases, the vapour will become more transparent for D_1 light. D_2 light shows the opposite effect: the transition probabilities for σ^+ light for level $-\frac{1}{2}$ and level $+\frac{1}{2}$ are in the ratio 1 : 3. Atoms in the $m = +\frac{1}{2}$ level absorb three times more σ^+ light than atoms in the $m = -\frac{1}{2}$ level. So if N_- decreases and N_+ increases as a result of pumping (by D_1 and by D_2 in pure vapour), the D_2 light will be more strongly absorbed. If both D_1 and D_2 transmitted by the vapour fall on the same detector, the resultant effect is not obvious. Either D_2 must be eliminated by an interference filter, or the two lines must be separated by a dispersive device and measured separately by two different photodetectors. In the latter case a differential detection method can be applied. For the measurement of the intensity of the transmitted light beam a simple photocell can be used.

If very small effects have to be measured – for example a radiofrequency resonance producing small population changes – a low-frequency modulation can be applied in connection with a narrow band a.c.-amplifier and a lock-in detector. By this technique the signal-to-noise ratio can be considerably improved. Changes of the order of 10^{-4} in the light intensity can be detected.

2.2.2. *Observation of the resonance radiation scattered at right angle from the direct light beam*

The pumping beam (σ^+ light) is propagated in the z-direction and a steady magnetic field can be applied in the z-direction (Fig. 11). The light absorbed by the atoms is reemitted spontaneously as resonance radiation in all directions of space. The resonance light emitted at right angle of the exciting beam has a definite intensity and a definite polarization depending on the Zeeman scheme of the pumping transitions. Consider again pumping by lines of type D_1 and D_2. If D_1 is used alone for pumping, we see that only atoms in the $m = -\frac{1}{2}$ state can absorb σ^+ photons. The number of photons absorbed (and reemitted) in unit time is proportional to N_-, number of atoms in the $m = -\frac{1}{2}$ state. If as a result of pumping the number of atoms N_- decreases, the intensity of the scattered light will decrease in the same proportion.

If both lines D_1 and D_2 are used together for pumping, and if they are of equal intensity, no change in the total intensity of the scattered

line can be seen as a result of change of the population N_- and N_+. But in this case, the population change can be monitored by examining the polarization of the scattered light. The photons absorbed by the atoms in the $-\frac{1}{2}$ state give rise to emission of π photons and of σ photons. The photons absorbed by the atoms in the $+\frac{1}{2}$ state (D_2 photons only) give rise to emission of σ photons only. As a result of pumping, the intensity ratio $\mathcal{I}_\sigma/\mathcal{I}_\pi$ increases.

The best way to measure this ratio is to use two photomultipliers equipped with polarizers receiving both the light scattered at right angle of the exciting beam: one isolating the π light vector $\|z$, the other isolating the σ light $\perp z$ (Fig. 11).

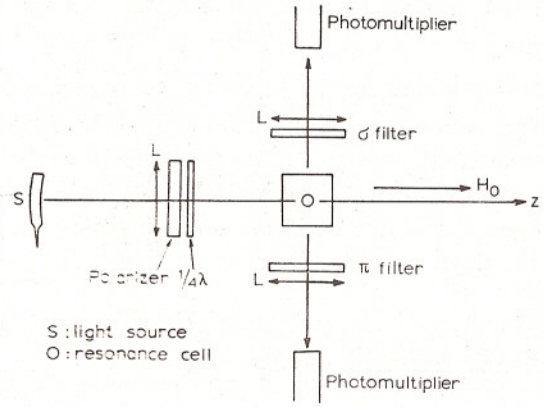

Fig. 11. Mounting of the detection method for measurement of intensity and polarization of the scattered resonance light.

The two photomultiplier signals can be matched in a differential mounting (BROSSEL [1952]).

This technique has been extensively used by the Paris group. The scattered resonance light is polarized only in the case of pumping in pure vapours. If a buffer gas of high pressure is present in the resonance cell, collisions will equalize the populations of the Zeeman levels of the excited state, and the resonance light will be unpolarized. In this case the polarization technique cannot be used.

2.2.3. *Use of secondary light beam to detect atomic orientation*

When atoms of a vapour are polarized or aligned along a z-axis by a primary light beam, the vapour is no more an isotropic medium but acquires properties of optical anisotropy, which can be demonstrated

by light whose frequency k is different from the absorption frequency k_0 of the atoms. Atoms polarized along the z-axis give rise to a strong paramagnetic Faraday effect for light that propagates parallel or nearly parallel the z-axis.

The sense of the Faraday rotation depends on the sign of the frequency difference $k-k_0$. This effect has been demonstrated by GOZZINI [1962] and can be used to measure the amount of atomic polarization (Fig. 12).

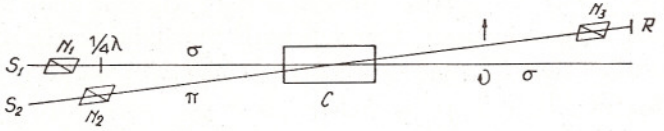

Fig. 12. Detection method for observation of the Faraday effect (GOZZINI [1962]).

Alignment of atoms along the z-axis (or polarization of a state $J>\frac{1}{2}$) causes birefringence of the medium for light that propagates in a direction perpendicular to the z-axis. Like the Faraday rotation this birefringence will change sign with the frequency difference $k-k_0$. This birefringence has not been observed actually, but can be used to measure the degree of alignment of a vapour.

2.2.4. *General scheme of an experiment of optical pumping. Steady-state signals and transient signals*

In absence of optical pumping the populations of different Zeeman levels of the ground state (without or with hyperfine structure) are given by the Boltzmann formula governing thermal equilibrium:

$$\frac{N_2}{N_1} = \exp\left(-\frac{E_2-E_1}{kT}\right) = \exp\left(-\frac{h\nu_{21}}{kT}\right).$$

N_2 and N_1 are the populations of levels E_2 and E_1 whose energy difference is $\Delta E = E_2-E_1 = h\nu_{21}$, where ν_{21} is the resonance frequency corresponding to the magnetic dipole transition between these two levels.

For ordinary temperature ($T = 300°$ K) the mean energy of thermal agitation kT is of the order of 0.025 eV or 200 cm^{-1} in the wave-number scale. Hyperfine intervals and Zeeman intervals in practically realizable fields are rarely larger than 1 cm^{-1} = 30 000 Mc/s, so that

$$\xi = \frac{\Delta E}{kT} \leqq \frac{1}{200}$$

and

$$\frac{N_1-N_2}{N_1+N_2} = \tfrac{1}{2}\xi \leqq \frac{1}{400}.$$

Compared to the population differences obtained by optical pumping the thermal equilibrium differences are quite negligible and in general beyond the possibility of measurement by optical-detection methods. Practically thermal equilibrium in a vapour at room temperature corresponds to equal populations of all ground-state Zeeman levels.

2.2.4.1. Steady-state signals

The distribution of ground-state sublevel population can be considerably changed by optical pumping. Relative population differences $(N_1-N_2)/(N_1+N_2)$ of the order of 0.3 to 0.8 are easily obtained and revealed by a substantial change of the light signal, either in the intensity of the signal of the pumping light transmitted or in the intensity and polarization signals of the scattered resonance light.

In steady-state conditions of relaxation and of optical pumping a definite steady-state distribution of population – what we call a dynamical equilibrium – is maintained and monitored by the light signal. If we apply to the atoms a radiofrequency field H_1 which induces magnetic resonance transitions, a new steady-state distribution is reached and maintained if the amplitude and the frequency of H_1 remain constant. This distribution depends on the amplitude of H_1 and on the frequency ω of the field applied and its relative position to the resonance frequency ω_0 of the atoms (which depends on the steady-field value H_0; for pure Zeeman transitions $\omega_0 = \gamma H_0$). At constant amplitude H_1 a magnetic resonance curve can be obtained by changing the difference $(\omega-\omega_0)$ (either by changing the frequency ω of the applied field or by changing the field value H_0).

This can be done point by point, and for each steady-state condition the signal can be read on a galvanometer connected to the photodetector. The resonance curves of Fig. 10 have been traced point by point by this method.

If the parameter ω (or ω_0) is swept continuously through resonance, the light signal is changed continuously.

Using this continuous sweep method, resonance curves can be traced on an oscilloscope and photographed. Figure 13 shows a picture of resonance curves taken in this way. It must be kept in mind that to ob-

tain a nondeformed curve corresponding to steady-state conditions, the sweep velocity must be slow, the time of sweep through a reso-

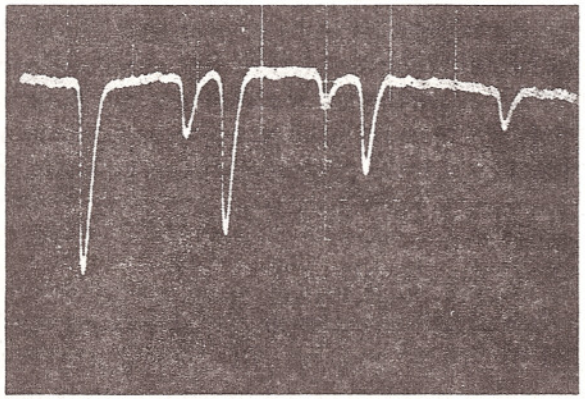

Fig. 13. Oscilloscope picture of the Zeeman transitions of the ground state of ^{23}Na (ANDERSON and RAMSEY [1963]).

nance curve being much longer than the relaxation time. Otherwise the curve will be deformed by transient effects.

2.2.4.2. Transient signals

Instead of waiting for establishment of steady-state conditions before making a measurement, or instead of using slow sweep which guarantees steady-state conditions every time, transient signals can be observed systematically. They are a powerful tool for studying the evolution of a spin system as a function of time.

The pioneer work in this direction is Franzen's study of optical pumping in rubidium-vapour (FRANZEN [1959]), investigating the effect of different buffer gases on the pumping efficiency and on the relaxation times. To obtain transient signals, the light signal corresponding to the intensity of the transmitted or the scattered light beam, is connected to the vertical scale of an oscilloscope while the oscilloscope spot is swept horizontally from left to right as a linear function of time. On the incident light beam, between the light source and the resonance bulb a shutter can be suddenly inserted or removed (commercial high-speed photographic camera shutters are convenient).

Figure 14 shows a photograph of the transient signal curve. The bottom-line on the left shows the zero-signal, the shutter being inserted.

At the time instant indicated by the arrow the shutter is suddenly removed, the light goes through the rubidium vapour and falls on the photocell. The signal is an increasing function of time, showing that

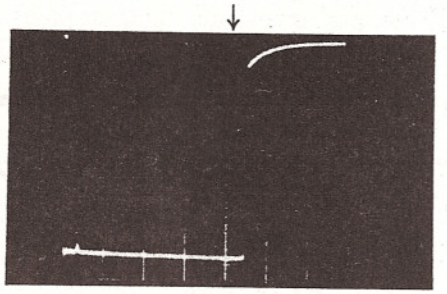

Fig. 14. Oscilloscope picture of the transient signal curve of light transmitted by Rb vapour (FRANZEN [1959]).

the vapour becomes more transparent as a result of the optical-pumping process. The steady-state conditions are approached exponentially.

Figure 15 shows the transient signal curve obtained by CAGNAC [1960] on optically pumped ^{199}Hg atoms by 2537 Å. This signal corresponds to the intensity of the light scattered at right angle. In this case the signal which is proportional to the number of atoms N_- in the $m = -\frac{1}{2}$ state is a decreasing function of time, showing that the state $m = -\frac{1}{2}$ is emptied by pumping. Let us solve the differential equations of § 2.1.2

$$\frac{dn}{dt} = \frac{N-n}{T_P} - \frac{n}{T_1}.$$

If we write

$$n_0 = \frac{N}{1+T_P/T_1} \quad \text{and} \quad \frac{1}{\tau_1} = \frac{1}{T_P} + \frac{1}{T_1}$$

we obtain the solution:

$$n = n_0(1-e^{-t/\tau_1})$$

or

$$N_- = \tfrac{1}{2}[N-n_0(1-e^{-t/\tau_1})]$$

which shows that N_- decreases from its thermal equilibrium value $\frac{1}{2}N$ exponentially to its asymptotic steady-state value $\frac{1}{2}(N-n_0)$ under pumping with the time constant τ_1.

A very elegant method has been initiated by Franzen to measure

directly the thermal relaxation time T_1. If we again insert the shutter for a short-time interval Δt as shown in Fig. 15, the atoms will relax partially during this darkness time with a time constant T_1 and then

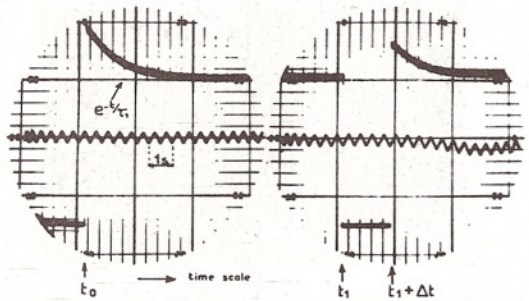

Fig. 15. Oscilloscope picture of the transient signal curve of resonance light scattered by ^{199}Hg vapour (CAGNAC [1960]).

pumping sets in again. Repeating this several times, but changing the darkness interval Δt and superposing the curves on the same photograph (enlarging also the vertical scale), we obtain a picture such as shown in Fig. 16 for the light transmitted by Rb atoms and in Fig. 17 for the light scattered by ^{199}Hg atoms.

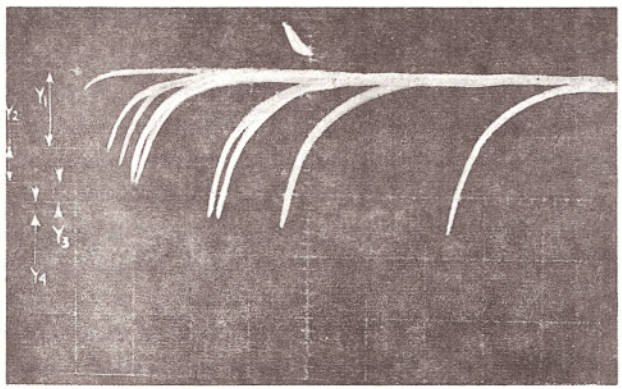

Fig. 16. Transient signals of light transmitted by Rb vapour. Construction of the T_1-relaxation curve (FRANZEN [1959]).

The envelope of the starting points lies on an exponential curve whose time constant is T_1. With the knowledge of T_1 and τ_1, we can now calculate the pumping time

$$\frac{1}{T_P} = \frac{1}{\tau_1} - \frac{1}{T_1}$$

which turns out to be of the order of 1 second in the case of mercury.

The transient signal method can also be applied to study the behaviour of the spins when a radiofrequency field H_1 at resonance is

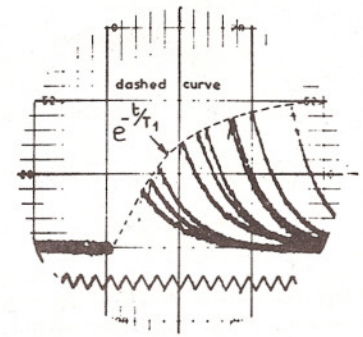

Fig. 17. Transient signals of light scattered by ^{199}Hg vapour. Construction of the T_1-relaxation curve (CAGNAC [1960]).

suddenly applied. Instantaneously all oriented spins will begin to nutate in phase. Their motion can be described classically in the rotating frame as a precession of the macroscopic magnetization vector $\langle M \rangle$ around an 'effective field'

$$H_e = [H_1^2 + (H_0 - \omega/\gamma)^2]^{\frac{1}{2}},$$

with a precession frequency $\omega' = [\omega_1^2 + (\omega_0 - \omega)^2]^{\frac{1}{2}}$, where ω_1 is defined as $\omega_1 = \gamma H_1$ (ABRAGAM [1961], ch. IIA).

The population excess $n = N_+ - N_-$ oscillates according to the Rabi formula:

$$n = n_0[1 - 2(H_1/H_e)^2 \sin^2(\tfrac{1}{2}\omega' t)].$$

At exact resonance $\omega = \omega_0 = \gamma H_0$, H_e reduces to H_1 and ω' to ω_1 and the Rabi formula becomes

$$n = n_0[1 - 2\sin^2(\tfrac{1}{2}\gamma H_1 t)].$$

These oscillations give rise to oscillations of the scattered (or transmitted) light which appear on the transient signal (Fig. 18). The figure shows that these oscillations are damped. Damping occurs because the nutating atoms relax and because new atoms that are optically pumped

begin to nutate with different phase. It has been shown by CAGNAC [1960] that the damping constant of the sinusoid is given by

$$\frac{2}{\tau'} = \frac{1}{\tau_1} + \frac{1}{\tau_2}.$$

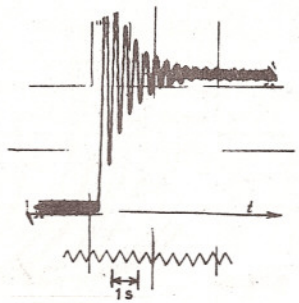

Fig. 18. Transient signals of light scattered by ^{199}Hg vapour. Sudden application of the H_1 radiofrequency field. Nutation signal (CAGNAC [1960]).

It depends on the longitudinal orientation time τ_1, and on the transverse relaxation time τ_2 in presence of pumping light. From the sinusoid spacing at resonance, ω_1 can be determined. This leads to an absolute measurement of $H_1 = \omega_1/\gamma$.

Figure 19 shows that the sinusoid becomes asymmetric when we go out of resonance ($\omega \neq \omega_0$), according to the general Rabi formula.

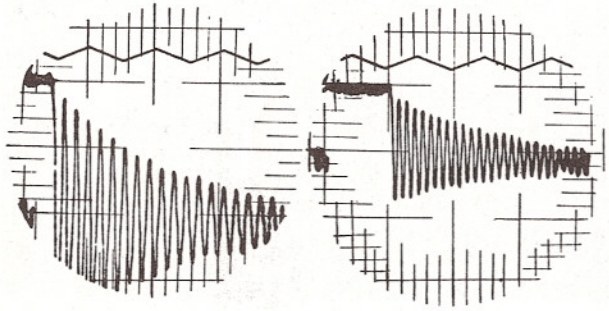

Fig. 19. Transient nutation signals, off resonance (CAGNAC [1960]).

The damping of the sinusoid leads to the steady-state values corresponding to the measured magnetic resonance signal as already described. Only at exact resonance and for strong H_1 field is the population excess n completely destroyed and 'saturation' is obtained.

These radiofrequency transients observed optically are analogous to those observed by TORREY [1949] with the conventional radiofrequency detection method.

Other interesting transient signals can be observed: after orienting optically atoms by circularly polarized light in a small steady field H_0 parallel to the light beam, the field H_0 may be suddenly reversed (DEHMELT [1957a]). The spin polarization, following adiabatically the field, will reverse also, and a strong sudden light signal-change will be observed, corresponding to the change of $+n_0$ to $-n_0$.

After this change, the initial light signal will be exponentially restored with the pumping-time constant τ_1. The observation of this 'reversal signal' provides a simple method to estimate the polarization degree n_0.

2.3. CHARACTERISTIC FEATURES OF OPTICAL PUMPING METHODS

Among the methods of atomic physics and especially among the methods of studying magnetic resonance, the optical-pumping methods have characteristic features which we want to emphasize.

Light has several functions: First of all, it is used for its 'pumping function' to obtain large changes of populations. Secondly, it is used for its 'detection function', these population changes being monitored by an optical light signal. Thirdly it must be mentioned that light has still another effect: it modifies the relaxation process and influences the time constant with which an atomic system reaches a steady-state equilibrium. The time constant τ_1 (in presence of light) is different from the time constant T_1 (in absence of light). Light acts also on the transverse relaxation time T_2 and changes it to τ_2. This can be easily understood by the fact that a radiofrequency field produces a coherent superposition of atomic states. Every process which interrupts this coherent superposition contributes to the relaxation: collisions do so, but so does also absorption of light, which takes away atoms from the ground state and shortens the life-time of ground-state atoms. We will see later on that presence of light produces also an imaginary relaxation term, which corresponds physically to a change of resonance frequencies and to a displacement of atomic energy levels.

A characteristic feature of optical detection of radiofrequency resonance is the fact that it constitutes a 'trigger detection'. Changes in the atom, induced by small energy photons of a radiofrequency field, give rise to changes – at a quantum yield unity involving high-energy optical photons.

A nuclear magnetic resonance transition in ^{199}Hg, produced by a photon of frequency 10^3, is followed by absorption of an ultraviolet photon of frequency 10^{15}. In this conversion process the atom itself acts as a quantum amplifier, the amplification factor being 10^{12} — corresponding to 120 decibels.

As high-energy photons can be more easily detected than radiofrequency photons, this explains why the sensitivity of the optical-detection method is much higher than the sensitivity of radiofrequency detection where the radiofrequency energy transfer is measured directly.

The optical method enables us to observe pumping, relaxation and resonance effects on matter in a very diluted state. An extreme case is optical pumping of mercury vapour by the resonance line 1850 Å. Good resonance signals can be observed in a resonance bulb of 10 cm^3, the mercury drop on the reservoir being at a temperature of $-50°C$. At this small vapour-pressure (10^{-6} mm Hg) the number of atoms in the cell is less than 10^{11}. This is a quantity of the order of 10^{-11}g.

Rare isotopes available in small quantities only, especially radioactive isotopes can be studied and their nuclear properties can be investigated.

2.4. LONGITUDINAL AND TRANSVERSE QUANTITIES: 'COHERENCE'

Up to now, we have described the ensemble of atoms by the populations of the different Zeeman sublevels in the ground state: Large differences of population may be achieved by optical pumping; any change of them may be optically detected by monitoring the absorbed or re-emitted light.

As we have seen, simple physical quantities may be connected to these differences of population. When the atom has only two Zeeman sublevels in the ground state (we will come back to the general case at the end of this section), the population difference between the two sublevels is directly proportional to the macroscopic *longitudinal* magnetization, $\langle M_z \rangle$, of the vapour (parallel to the magnetic field H_0).

So, we are naturally led to ask the following two questions about the macroscopic *transverse* magnetization $\langle M_\perp \rangle$ (perpendicular to H_0): Is it possible to build up by optical pumping a macroscopic transverse magnetization? Is it possible to detect optically the variation of this physical quantity?

2.4.1. *Transverse optical pumping*

Let us start with a simple remark concerning the polarization that the light beam must have in order to achieve a transverse pumping: If, at thermal equilibrium, $\langle M_\perp \rangle = 0$, this is due to the fact that there is no privileged transverse direction. The direction of the individual transverse magnetization of each atom varies in a random way from one atom to another so that the net resultant is zero. The situation remains unchanged if the electric field of the light beam does not favour any transverse direction. This is the case for the three polarizations σ^+, σ^-, π (defined with respect to H_0) which, consequently, must be excluded in a transverse optical-pumping experiment. All the experiments we will describe now correspond to the following situation. Let Oz be the direction of the field H_0 with the light beam being propagated along Ox and having a right circular polarization with respect to this direction (Fig. 20).

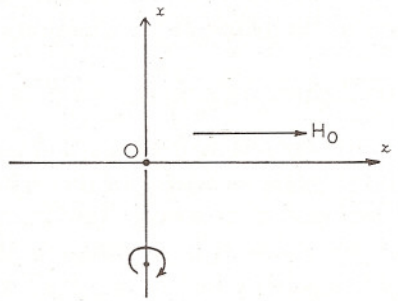

Fig. 20. Scheme for transverse optical-pumping.

2.4.1.1. Transverse pumping in a weak magnetic field

The magnetic dipole of an atom which has been just pumped by the light beam of Fig. 20, is pointing along the Ox direction. Immediately afterwards it begins to precess around H_0 at the Larmor frequency of the ground state ν_f. This precession does not last indefinitely. After a mean time θ, the atom undergoes a disorientating collision or absorbs another photon and its orientation is destroyed or changes completely.

In order to obtain the whole transverse magnetization of the vapour at a given time t_0, we have to take the resultant of all the dipoles which have been pumped at a time $t < t_0$ and which have not yet undergone a disorientating process at time t_0. All these dipoles form a kind of a fan, starting from the Ox-axis and having an average angular spread of the order of $2\pi\nu_f\theta$. If $2\pi\nu_f\theta \ll 1$, this angular spread is very small;

the resultant has its maximum value and is directed along Ox. When ν_f increases, the fan opens, the resultant decreases, and rotates: a $\langle M_y \rangle$-component appears. When $2\pi\nu_f\theta \gg 1$, the fan has become isotropic in the plane perpendicular to H_0 so that the resultant is now zero. This phenomenon can be analysed in a quantitative way. One finds that $\langle M_x \rangle$ (and $\langle M_y \rangle$) varies versus $\nu - \nu_f$ as an absorption (and a dispersion) curve; the half width being $\Gamma' = (2\pi\theta)^{-1}$,

$$\langle M_x \rangle \simeq \frac{\frac{1}{2}\Gamma'^2}{(\nu-\nu_f)^2+(\frac{1}{2}\Gamma')^2},$$

$$\langle M_y \rangle \simeq \frac{\Gamma'(\nu-\nu_f)}{(\nu-\nu_f)^2+(\frac{1}{2}\Gamma')^2}.$$

These predictions have been confirmed experimentally on the odd isotopes of Cd (LEHMANN and COHEN-TANNOUDJI [1964a]). This phenomenon is very similar to the Hanle effect (MITCHELL and ZEMANSKY [1934], p. 262) which appears in the excited state (magnetic depolarization; rotation of the plane of polarization).

2.4.1.2. Transverse pumping with modulated light

From the preceding discussion it seems that transverse pumping is possible only in very weak magnetic fields ($\nu_f\theta \ll 1$). An ingenious method proposed by BELL and BLOOM [1961] permits to remove this restriction. The method consists in modulating the light intensity at a frequency ν close to ν_f. To make the analysis simple, we will suppose that the light source emits light only by very short pulses, with a repetition frequency ν.

Let (T) be a frame $OXYZ$, the OZ-axis of which coincides with Oz. (T) rotates around Oz at a frequency ν. Let us begin to analyse the problem in (T). Suppose that OX and Ox coincide during a light pulse. The same holds true for the other pulses as (T) rotates at frequency ν. So, in (T), the dipoles will be always pumped in OX-direction. On the other hand, they precess in (T) at the frequency $\nu_f - \nu$. We are thus led in (T) to the same problem as above, provided that we replace ν_f by $\nu - \nu_f$: At a stationary state, there appears in (T) a net transverse magnetization which is fixed in direction and which is important only if $|\nu-\nu_f| \lesssim \theta^{-1}$. It is maximum for $\nu = \nu_f$ and zero for $|\nu-\nu_f| \gg \theta^{-1}$. Coming back from (T) to $Oxyz$, we see that transverse pumping with a modulated light at frequency ν builds up a net transverse magnetization rotating at the same frequency ν, provided that ν is sufficiently close to ν_f. The experiment has been successfully performed on alkali atoms by BELL and BLOOM [1961].

One of us suggested to extend this method to excited states (KASTLER [1961]). In this case, the light has to be modulated at a frequency close to the Larmor frequency ν_e of the excited state. The experiment has been successfully performed on Cd by ALEKSANDROV [1963]. Pebay-Peyroula has observed similar effects, using an electronic bombardment, modulated at the frequency ν_e, the electron beam being perpendicular to H_0 (NEDELEC *et al.* [1963]).

The following remark may be made concerning the two experiments described above: In the experiment described in § 2.4.1.1, the light beam tends to transfer to the atom transverse angular-momentum in the Ox direction, *in a static way*. But, for the atom, this physical quantity has a natural motion: It precesses at the frequency ν_f and is damped with a time constant θ. Thus this problem is formally quite analogous to the problem of the static excitation (at a frequency 0) of an oscillating circuit, having a natural frequency ν_f and a pass-band θ^{-1}. The result is well known: The excitation is appreciable only if the excitation frequency falls within the pass-band, i.e. if $|\nu_f - 0| \lesssim \theta^{-1}$. The same analogy may be used for the experiment described in § 2.4.1.2. We have now to excite at frequency ν the same oscillating circuit (natural frequency ν_f, pass-band θ^{-1}). A *'forced motion'* at frequency ν occurs, which is appreciable only if $|\nu-\nu_f| \lesssim \theta^{-1}$.

2.4.2. *Transverse detection. Cross-beam technique*

We will now describe an optical-detection method, proposed the first time by DEHMELT [1957b] and applied initially to the alkali atoms by BELL and BLOOM [1957]. This method provides optical signals which are directly proportional to the transverse physical quantities.

Two light beams are used. They are perpendicular and right circularly polarized (Fig. 21). The first beam propagates along H_0 (Oz) and *optically pumps* the vapour contained in the resonance cell O. The second beam, called cross beam, is a detection beam. (It is not modulated. H_0 is assumed to be sufficiently large so that no transverse pumping is possible.)

Being pumped by the first beam, the vapour gets a longitudinal magnetization $\langle M_z \rangle$. It is then possible to achieve the magnetic resonance with a radiofrequency field H_1, perpendicular to H_0, and rotating

around H_0 at a frequency ν, sufficiently close to ν_l. It is well known from Bloch's equation (BLOCH [1946]), that, at a stationary state, the total magnetization $\langle M \rangle$ is no longer parallel to Oz. It has a transverse

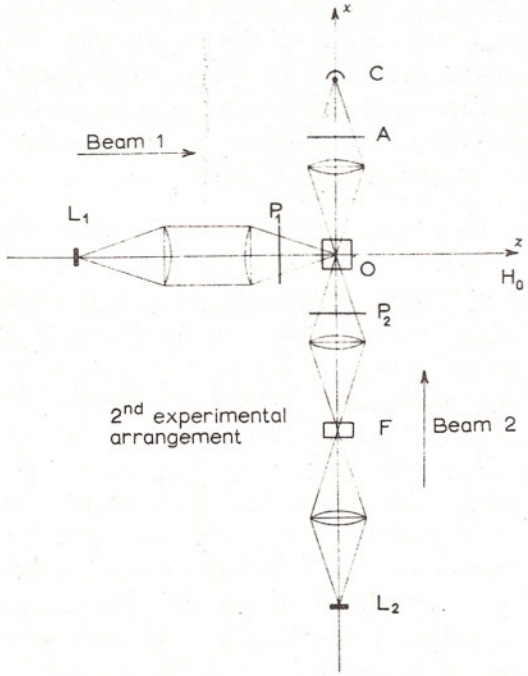

Fig. 21. Cross-beam detection method.

component $\langle M_\perp \rangle$, rotating at the same angular frequency as H_1. The amplitude and relative phase (with respect to H_1) of $\langle M_\perp \rangle$ depend on $\nu - \nu_l$. (It is H_1 which introduces here a privileged transverse direction and permits to have a transverse magnetization of the vapour as a whole.)

Let us now consider the absorption of the second beam by the vapour. We suppose that we study an alkali vapour and that the D_2 line emitted by the lamp of the second beam is suppressed by some filter. For simplicity, we neglect the nuclear spin. Let us consider the transition probabilities of the D_1 line as shown in Fig. 2. We see immediately that the absorption of the second beam is important when the atoms are in the eigenstate $|-\frac{1}{2}\rangle$ with respect to Ox, i.e. when the transverse magnetization is pointing in the negative direction of the Ox-axis; zero when the atoms are in the eigenstate $|+\frac{1}{2}\rangle$ with respect to Ox, i.e when the transverse magnetization is pointing in the positive direction of the Ox-axis. So the importance of the absorption depends on the

value and the sign of $\langle M_x \rangle$. As $\langle M_\perp \rangle$ rotates around H_0 at frequency ν, $\langle M_x \rangle$ is modulated at the same frequency. So, there appears in the photoelectric current of the photocell C (which measures the absorption of the second beam) a component modulated at frequency ν and directly proportional to $\langle M_\perp \rangle$. This is indeed a transverse detection as the optical signal is proportional to a transverse physical quantity.

Figures 22 and 23 represent some experimental results (COHEN-TANNOUDJI [1962a]). The element studied here is not an alkali but ^{199}Hg.

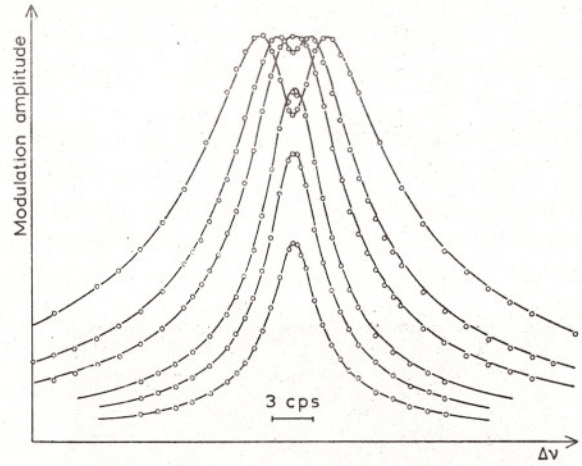

Fig. 22. Nuclear magnetic resonance curve of ^{199}Hg taken by the cross-beam technique (COHEN-TANNOUDJI [1962a]).

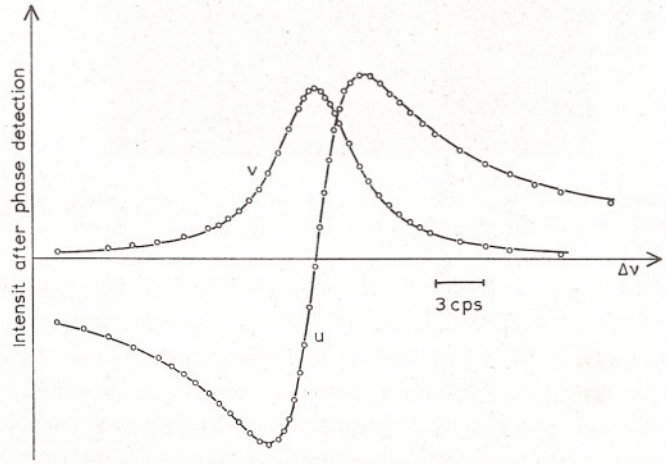

Fig. 23. u-component and v-component of the signal shown in Fig. 22. The components are separated by a phase-detection method.

The hyperfine component $i = \frac{1}{2} \rightarrow F = \frac{1}{2}$ which is excited selectively by the second beam has the same structure as the D_1 line of an alkali without nuclear spin. Figure 22 shows how the amplitude of the modulation, i.e. $|\langle M_\perp \rangle|$, varies with $\nu - \nu_1$ for different values of the amplitude, H_1, of the radiofrequency field. It is also possible to do a phase detection and to detect either the component in phase with H_1, u, or the component in quadrature, v. u and v vary respectively with $\nu - \nu_1$ as a dispersion and an absorption curve. This appears clearly on Fig. 23. (The curves of Figs. 22 and 23 are curves predicted by theory; the points represent results of experiments. The value of the parameter corresponding to the sensitivity of the apparatus has been adjusted on one point.)

With such modulated signals it is also possible to study some transient phenomena, for example those which appear when the radiofrequency field is cut off suddenly. One obtains in this way a free-precession signal (Fig. 24) which is very useful for studying the damping of the transverse magnetization by the relaxation processes. Let us remark that

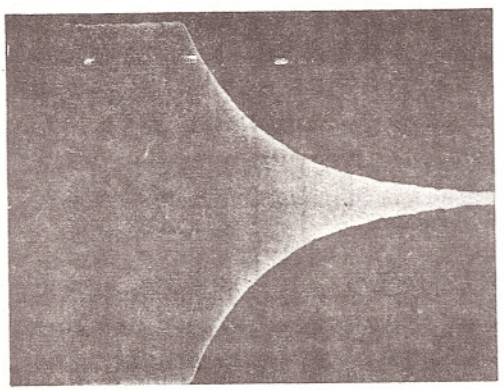

Fig. 24. Modulation signal of the cross beam for ^{199}Hg. Free-decay signal after cutoff of H_1 and of the primary light beam (COHEN-TANNOUDJI [1962a]).

such a signal is quite similar to the one obtained in the radioelectric methods of detection, which make use of the electromotive force induced in a coil by the rotation of the whole transverse magnetization. It is therefore possible, and this has been done, to extend to the optical methods a series of techniques developed for radioelectric methods, for example the techniques which make use of radiofrequency pulses ($\frac{1}{2}\pi$ pulses, π pulses, sequences of pulses . . .).

Finally, it is possible to observe the anomalous dispersion of the

vapour rather than the absorption. Suppose that the second beam is linearly polarized; when it passes through the vapour, the plane of polarization of this beam undergoes a rotation proportional to $\langle M_x \rangle$ (transverse paramagnetic Faraday effect). As $\langle M_x \rangle$ is modulated at the frequency ν, it follows that the rotation of the plane of polarization is modulated at the same frequency and this can be detected by putting an analyser before the photocell. This effect has been observed on ^{199}Hg (MANUEL and COHEN-TANNOUDJI [1963]). The optical frequencies of the second beam, k, may differ considerably from the resonant optical-frequency, k_0, for anomalous dispersion decreases with $k_1 - k_0$ much more slowly than absorption. The possibility of using a second beam, for which the absorption is negligible, is very important from a practical point of view because, as we shall see later, optical absorption broadens magnetic-resonance curves in the ground state.

2.4.3. *Generalization – Notion of coherence*

After having described some experiments with very simple physical pictures, we will now approach the problem in more general terms.

Let $|E\rangle$ be the different energy eigenstates of the atom. The more general state in which the atom can be found is a linear superposition of the $|E\rangle$ states

$$|\psi(t)\rangle = \sum_E a_E(t)|E\rangle.$$

All physical predictions concerning the atom in the state $|\psi\rangle$ may be expressed in terms of the complex numbers $a_E(t)$. For example, the mean value in the state $|\psi\rangle$ of a certain physical quantity G (with matrix elements $G_{EE'}$) is

$$\langle G \rangle = \sum_{EE'} a_E(t) a^*_{E'}(t) G_{E'E}.$$

Instead of the $a_E(t)$, it is more convenient to introduce the quantities $\sigma_{EE'} = a_E(t) a^*_{E'}(t)$. The σ matrix is the density matrix. One has

$$\langle G \rangle = \sum_{EE'} G_{EE'} \sigma_{E'E}$$
$$= \text{Sp. } \sigma G.$$

If G does not commute with the energy, i.e. if the non-diagonal elements $G_{EE'}$ $(E' \neq E)$ are not all zero, one sees that G depends in general on the non-diagonal elements of the density matrix. In the absence of perturbation, the Schrödinger equation gives immediately the evolution of the density-matrix elements:

$$\sigma_{EE'}(t) = \exp\left[-i((E-E')(t-t_0)/\hbar)\right]\sigma_{EE'}(t_0).$$

Let us now consider an ensemble of identical atoms. According to statistical mechanics the correct description of this ensemble is contained in a total density-matrix, which is the average of the individual density-matrices representing each atom. The diagonal elements of this total density-matrix G_{EE} represent the mean probability for an arbitrary element of the ensemble being in the state $|E\rangle$. They are the populations of the different energy levels. When a non-diagonal element $\sigma_{EE'}$ of this total density matrix is different from zero, there is a same cause, common to all atoms, which is responsible for the fact that the relative phase of $a_E(t)$ and $a_{E'}(t)$ does not change in a random way from one atom to another, so that averaging $a_E a_{E'}^*$ over all atoms does not give zero. When this is the case, we shall say that there is 'coherence' between the states $|E\rangle$ and $|E'\rangle$ and we shall call by convention the quantity $\sigma_{EE'}$ coherence between the states $|E\rangle$ and $|E'\rangle$ (COHEN-TANNOUDJI [1962a, b]). Some physical quantities G which do not commute with energy and which depend on $\sigma_{EE'}$ have then a behaviour which reveals the existence of such a coherence. If, for example, the evolution of the system develops freely, the motion of $\langle G\rangle$ comprises a component modulated at frequency $(E-E')/\hbar$. Such a behaviour cannot be understood if one describes the ensemble of atoms only in terms of populations.

In the experiments described above, we have supposed, for simplicity, that there were only two Zeeman sublevels $\pm\frac{1}{2}$ in the ground state. In that case, there is only one non-diagonal element $\sigma_{\frac{1}{2},-\frac{1}{2}}$ ($\sigma_{\frac{1}{2},-\frac{1}{2}} = \sigma^*_{-\frac{1}{2},\frac{1}{2}}$). The modulus and argument of $\sigma_{\frac{1}{2},-\frac{1}{2}}$ represent respectively the magnitude of $\langle M_\perp\rangle$ and its orientation in the plane perpendicular to H_0. In the general case, there are more than two energy sublevels and several types of coherence have to be considered: 'Zeeman coherences', when $|E\rangle$ and $|E'\rangle$ are two Zeeman sublevels of the same hyperfine level; 'hyperfine coherence', when $|E\rangle$ and $|E'\rangle$ belong to two different hyperfine levels. The evolution frequencies of these coherences, $(E-E')/h$, fall in the hertzian range. So, we will call these types of coherence 'hertzian coherence'.

It would also be possible to consider the case where $|E\rangle$ belongs to the ground state of the atom, and $|E'\rangle$ to the excited one. $\sigma_{EE'}$ is then an 'optical coherence'. The physical quantity related to $\sigma_{EE'}$ is the electric dipole of the atom which oscillates at the optical frequency $(E'-E)/h$. Optical coherence may exist only if the phase of the vibration of the different electric dipoles does not vary in a random way from one atom to another, i.e. if the ensemble of atoms is driven by a light wave sufficiently coherent (in the optical sense) in time and space. With the usual light sources, such a situation is far from being realized and we may neglect optical coherence. With a laser as a light source, this is no longer the case.

From what has been said above we may conclude by saying, that, in several cases, an ensemble of atoms cannot be described only in terms of the populations of the different energy eigenstates. One has also to take into account the non-diagonal elements of the density matrix. As has been shown on definite examples these quantities can play an important role in the optical pumping experiments. New optical properties appear when the ensemble of atoms possesses hertzian coherence. Clearly, a complete theory of the optical-pumping cycle must give the evolution under the effect of optical pumping of all the elements—diagonal as well as non-diagonal ones—of the density matrix representing the ensemble of atoms. We will return to this problem later.

Finally let us remark that we have restricted ourselves in this section to the study of ground states. Several effects depending on hertzian coherence exist also for excited states. We will just enumerate them: the Hanle effect (MITCHELL and ZEMANSKY [1934]), level crossing (COLEGROVE *et al.* [1959], FRANKEN [1961]), light beats (DODD *et al.* [1959], BARRAT [1961]), coherent multiple scattering (GUIOCHON *et al.* [1957], BARRAT [1959]). (It was coherent multiple scattering which first raised the problem of the emission of light energy by an atom which is in a coherent superposition of Zeeman sublevels.)

§ 3. Results obtained by Optical Pumping

3.1. INTRODUCTION

In developing the principles of optical pumping, we have already mentioned its applications. We may consider now some of them in more detail:

Optical pumping leads to a simple device to study radiofrequency resonance, to investigate Zeeman intervals and hyperfine intervals. From the resonance positions atomic and nuclear properties can be deduced, such as: g factors, nuclear moments, hyperfine constants, hyperfine anomalies, frequency shifts produced by foreign gas collisions, etc.

From the width of the resonance lines and from the transient signals, relaxation times T_1 and T_2 can be evaluated, and the mechanisms of the relaxation processes can be elucidated.

Since in the diluted vapour state, relaxation occurs principally on the walls, the study of this relaxation leads to interesting results concerning surface physics.

Optical pumping leads to a systematic study of the interactions of atoms with electromagnetic fields in the optical range and in the radiofrequency range. New features of this interaction are brought out such as:

Multiple quantum transitions, coherence effects, displacements of energy levels by light.

Finally optical pumping gives rise to important technical applications: construction of sensitive magnetometers and of transportable frequency standards. We shall now review these different applications.

3.2. RADIOFREQUENCY SPECTROSCOPY BY OPTICAL PUMPING

Optical pumping permits to build up a simple and cheap device to investigate radiofrequency resonance in atomic systems.

The experimental equipment needed is: a stable light source, light filters and polarization screens, quarter wave plates, a temperature-controlled resonance bulb, a photodetector connected to a galvanometer, or to a lock-in amplifier and an oscilloscope screen, a Helmholtz coil producing a steady magnetic field of good homogeneity in space and good stability in time, and finally a radiofrequency circuit of high-frequency stability, a frequency meter and a radiofrequency power meter.

The centers of the resonance lines can be measured with high precision. In favourable cases a relative precision of $\Delta\nu/\nu = 10^{-6}$ for Zeeman resonances has been obtained. To deduce g factors and magnetic moments not only the resonance frequency but also the steady-field value H_0 has to be measured with precision.

The best way to do this is to calibrate the field by a conventional proton resonance.

For *pure Zeeman transitions* g factors are related to the field value and to the resonance frequency by the formula: $\nu = g(\mu_B/h)H$ for electron spin resonance (μ_B = Bohr magneton) or by the equivalent formula $\nu = g(\mu_n/h)H$ for nuclear resonance (μ_n = nuclear magneton).

In the latter case, the nuclear magnetic moment in units μ_n is defined as $\mu/\mu_n = ig$ where i is the nuclear spin number.

Among the results of measurements on pure Zeeman intervals, we may mention the comparison made by DEHMELT [1958] of the g_j factor of Na atoms in their ground state $3^2S_{\frac{1}{2}}$ and the g_e factor of the spin resonance of free electrons polarized by exchange collisions in optically pumped sodium vapour. Dehmelt has found the ratio g_j/g_e equal to unity with an accuracy estimated to 3×10^{-5}.

Dehmelt's experiment has been repeated by HOBART [1962] who attained an accuracy of 4×10^{-6} and gives the result

$$\frac{\mu_e(\text{Na})}{\mu_e(\text{free})} = 0.999\,982 \pm 4\times10^{-6}.$$

Hobart has found evidence for a shift of the free electron resonance produced by spin exchange collisions. This shift is proportional to the Na magnetization and changes sign with the sign of this magnetization. We will return to this question later on (BALLING *et al.* [1964]).

Another high-precision result is the measurement by CAGNAC [1960] and coworkers (LEHMANN and BARBÉ [1963]) of the nuclear magnetic moments of ^{199}Hg and of ^{201}Hg:

$$\mu_{199} = +\,0.497\,865 \pm 6\times10^{-6}\mu_n$$

$$\mu_{201} = -\,0.551\,344 \pm 9\times10^{-6}\mu_n.$$

These values have been calculated without making the diamagnetic correction. Their ratio has been measured with a very high accuracy:

$$\mu_{201}/\mu_{199} = -1.107\,416\,4 \pm 5\times10^{-7}.$$

The study of radioactive isotopes of mercury has been undertaken successfully by the M.I.T. group. WALTER [1962] has found for ^{197}Hg (65^H) the values $\mu_{197}/\mu_{199} = 1.042\,479 \pm 15\times10^{-6}$ leading with Cagnac's value for ^{199}Hg to $\mu_{197} = 0.519\,014 \pm 10\times10^{-6}\,\mu_n$ and STAVN [1963] has found for ^{195}Hg (9.5^H) the value $\mu_{195}/\mu_{199} = 1.070\,356 \pm 66\times10^{-6}$ leading to $\mu_{195} = 0.532\,892 \pm 33\times10^{-6}\,\mu_n$. The nuclear moments of ^{111}Cd and ^{113}Cd are being measured by LEHMANN (LEHMANN and BROSSEL [1964]).

Hyperfine intervals can be measured directly by observing the hyperfine transitions $\Delta F = 1$ in zero field or better by using a small field of the order of 10^{-2} gauss, to isolate the $\Delta F = 1$, $m_F : 0 \to 0$ transition from the other field sensitive $\Delta F = 1$ transitions (BELL and BLOOM [1958], ARDITI and CARVER [1958a], BENDER *et al.* [1958], BEATY and BENDER [1958]). Hyperfine intervals can also be evaluated indirectly

from the non-linear evolution of the Zeeman resonances $\Delta F = 0$ in intermediate fields.

The departure from linearity corresponds to the decoupling of nuclear spin and electron spin (Back–Goudsmit effect).

Hyperfine intervals already known have been re-measured by optical-pumping techniques for all alkali atoms except lithium and francium, and (by the exchange-collision method) for the three isotopes ^{1}H, ^{2}H and ^{3}H of hydrogen†.

The hyperfine intervals in the ground state $^4S_{\frac{3}{2}}$ have been measured by the exchange-collision technique for

$$^{14}N(i = 1), \qquad ^{15}N(i = \tfrac{1}{2}) \qquad \text{and} \qquad ^{31}P(i = \tfrac{1}{2})\dagger.$$

Table 2 gives a review of hyperfine intervals measured by optical-pumping techniques.

TABLE 2

$^4S_{\frac{3}{2}}$	Frequencies	Hyperfine constants
^{14}N	$\nu_{\frac{5}{2}\to\frac{3}{2}} = 26.127\ 21$ Mc/s	$A_{14} = 10.450\ 91$ Mc/s
$i = 1$	$\pm 18\times10^{-5}$	$\pm 7\times10^{-5}$
	$\nu_{\frac{3}{2}\to\frac{1}{2}} = 15.676\ 46$ Mc/s	$B_{14} = -0.000\ 05$ Mc/s
	$\pm 12\times10^{-5}$	$\pm 8\times10^{-5}$
^{15}N	$\nu_{2\to1} = 29.291\ 36$ Mc/s	$A_{15} = -14.645\ 68$ Mc/s
$i = \frac{1}{2}$	$\pm 16\times10^{-5}$	$\pm 8\times10^{-5}$
^{31}P	$\nu_{2\to1} = 110.111\ 382$ Mc/s	$A_P = 55.055\ 691$ Mc/s
$i = \frac{1}{2}$	$\pm 16\times10^{-6}$	$\pm 8\times10^{-5}$

The study of the hyperfine resonance $\Delta F = 1$, m_F: $0 \to 0$ of optically oriented atoms in different buffer gases has revealed important *frequency displacements* proportional to the buffer-gas pressure, depending on the nature of the buffer gas and on the temperature (Fig. 25).

Table 3 gives a review on the measurements made on these displacements. The displacements are positive for light buffer gases of small polarizability (He, H_2, N_2, Ne). They become negative for heavy buffer gases of high polarizability (Ar, Kr, Xe).

The theory of these displacements has been worked out by Margenau and coworkers (MARGENAU [1959], ROBINSON [1960], CLARKE [1962]) and by Adrian (ADRIAN [1960, 1962]).

† The references are given in Table 3.

These displacement effects are due to two types of interaction during the collisions of the paramagnetic atom with the diamagnetic buffer-gas molecule:

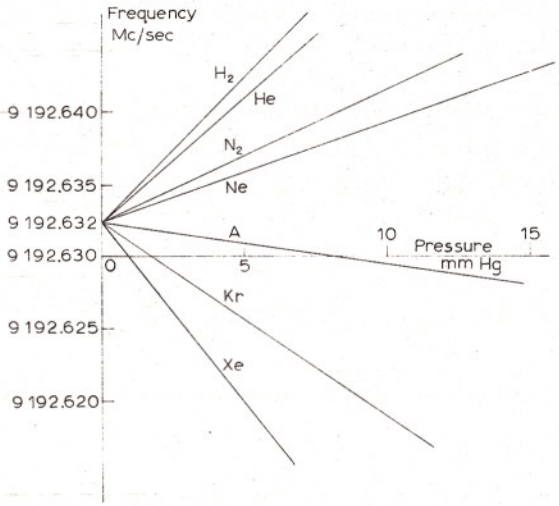

Fig. 25. Pressure shift of zero-field hyperfine resonance line of ^{133}Cs for different buffer gases (ARDITI and CARVER [1958b]).

1°) The Pauli exchange repulsion forces which tend to increase the electron density at the nucleus. This results in an increase of the hyperfine splitting and produces a positive displacement.

2°) The Van der Waals attraction forces which tend to reduce the electron density at the nucleus. This results in a decrease of the hyperfine splitting and produces a negative displacement. This latter effect is proportional to the polarizability of the buffer-gas molecule.

Both effects occur simultaneously: for highly polarizable buffer-gas molecules (Ar, Kr, Xe) the second effect predominates and the total shift is negative, whereas in the lighter gases this effect is overcome by the exchange effect and the resultant displacement is positive.

An interesting case is that of the nitrogen atom, where it has been shown that argon produces positive shifts. In this case, as has been emphasized by ADRIAN [1962], both effects produce a positive shift: the ground state of the N atom is indeed a $^4S_{\frac{3}{2}}$ $(2s)^2$ $(2p)^3$ state. The Van der Waals interaction mixes to it a small amount of the excited state $(2s)^1(2p)^4$. According to the Pauli exclusion principle the 2s electron excited to the 2p state must have its spin opposite to that of the three 2p electrons, and the electron remaining in the 2s state has the same

TABLE 3

Frequency shifts of $\nu_{0,0}$ hyperfine transition by buffer gas (in c/s/cm Hg)

Paramagn. species	$\nu_{0,0}$	He	H_2	N_2	Ne	Ar	Kr	Xe
^{23}Na	1771.626 2 Mc/s (ARDITI [1960])			+1 000	+800	0		
^{39}K	461.719 690 Mc/s (BLOOM and CARR [1960a])	+430 (65 °C)	+330		+240	−4	−420	
^{87}Rb	6 834.682 608 Mc/s (BENDER *et al.* [1958])					−520		
^{133}Cs	9192.632 Mc/s (ARDITI and CARVER [1958a])	+12 000		+8 500	+6 000	−2 000	−13 000	−23 500
^{1}H	1420.405 749 Mc/s (PIPKIN and LAMBERT [1962])	+48	−5.6		+28.8	−47.7		
^{2}H					+10.6	−14.8		
^{3}H	1516.701 477 Mc/s (PIPKIN and LAMBERT [1962])				+32.4	−50.5		
^{14}N	26.127 330 Mc/s ($\frac{1}{2} \rightarrow \frac{3}{2}$)	+7		+41.2				
^{15}N	29.290 910 Mc/s (LAMBERT and PIPKIN [1963])	+8.7			+16	+54.7		
^{31}P	110.111 382 Mc/s (LAMBERT and PIPKIN [1962])	+72			+135			

spin orientation as the total spin. The unpaired electron spin-density at the nucleus is enhanced, and a positive displacement results which adds its effect to the exchange effect. The same is true for phosphorus.

In this connection the investigation of the hyperfine interval of N and P atoms in presence of krypton and xenon would be of great interest.

Table 3 gives in its second column the value of the hyperfine intervals $\nu_{0,0}$ obtained by extrapolation of the measurements in buffer gas to zero gas pressure. These values, obtained in a glass bulb, differ slightly from the values deduced from the atomic-beam measurements. This difference is due to a residual shift caused by the wall collisions.

This shift is proportional to the polarizability of the paramagnetic atom. It is negligibly small for H atoms on paraffine or on teflon coatings (KLEPPNER *et al.* [1962]).

3.3. STUDY OF RELAXATION PROCESSES

3.3.1. *The methods of investigation*

We have already seen in § 2.2, that *the steady-state signals* and the *transient signals* give us information on relaxation processes. The *magnetic-resonance curves* are characterized by their shape, their peak intensity and their width at half intensity. The peak intensity of these curves gives information on the longitudinal relaxation time T_1.

For a high-radiofrequency amplitude the curves are 'saturated', at the center of the line the populations of the two resonating levels are equalized. So the peak intensity is proportional to the population difference N_0 produced by optical pumping

$$N_0 = \frac{N}{1+T_P/T_1} \qquad \text{depends on } T_1.$$

The higher is T_1, the stronger will be the intensity of the resonance. The fact that for a constant pumping-light intensity the addition of foreign gases to an alkali vapour enhances strongly the intensities of the Zeeman resonances, shows that in presence of a foreign gas the relaxation time T_1 is highly increased (buffer-gas effect).

The comparison of the resonance intensities in a bulb without coating and in a bulb with coating shows also that the relaxation time becomes much larger when the glass walls are covered with a suitable coating.

The *width of the resonance lines* at half intensity gives information

on the transverse relaxation time of the spins, if this width is due to 'homogeneous broadening'.

In an inhomogeneous magnetic field the resonance lines may be broadened by the field inhomogeneity. To avoid this inhomogeneous broadening, homogeneous magnetic fields must be used. If this condition is fulfilled, the transverse relaxation times can be deduced from the line-width. We have seen that the line-width depends on the radiofrequency power and on the pumping-light intensity. Two extrapolations to zero H_1 and to zero-light intensity have to be made to get the true transverse relaxation time T_2 according to the uncertainty relaxation:

$$\Delta\omega_0 = \frac{1}{T_2}.$$

Light itself is a factor of relaxation. Light absorption shortens the life-time of the ground state of atoms. In the presence of light the line-width is given by

$$\Delta\omega = \frac{1}{T_2} + \frac{1}{\theta_2}$$

where $1/\theta_2$ is the relaxation rate produced by light.

The recording of the *transient signals* permits to study the longitudinal and the transverse relaxation processes in a simple and elegant way.

We have already discussed Franzen's technique which leads to the plotting of the relaxation curve 'in the dark', from which T_1 can be directly deduced.

The *cross-beam technique* discussed in § 2.4.2. and especially the recording of the free-precession decay curve of $\langle M_\perp \rangle$ after a 90° pulse leads directly to the knowledge of τ_2, which depends still on the cross-beam light intensity:

$$\frac{1}{\tau_2} = \frac{1}{T_2} + \frac{1}{\theta_2}.$$

An extrapolation to zero-light intensity leads to $1/T_2$, relaxation rate produced by thermal relaxation in the dark.

This extrapolation can be avoided by using a cross-beam detection technique working on virtual transitions and measuring the Faraday rotation (MANUEL and COHEN-TANNOUDJI [1963]). In this case, there is no light absorption and the decay signal of $\langle M_\perp \rangle$ gives directly T_2.

The optical cross-beam technique keeps its sensitivity at very low precession-frequencies. For the study of nuclear relaxation of ^{199}Hg, COHEN-TANNOUDJI [1962] has used frequencies of 770 c/s and obtained signals with an excellent signal-to-noise ratio.

We have already mentioned the application of pulse techniques to the optical-detection method. We have seen that after a 90° pulse the decay of the free-precession signal leads to the measurement of τ_2. The longitudinal orientation time τ_1 can also be measured on the cross-beam signal, by using successive 180° pulses.

Each such pulse produces an instantaneous cross-beam signal proportional to $\langle M_z \rangle$ (the reversal of $\langle M_z \rangle$ by nutation gives rise to an intermediate $\langle M_\perp \rangle$ seen on the cross-beam modulation).

After the 180° pulse $\langle M_z \rangle$ recovers its original direction exponentially with time constant τ_1. If after the first 180° pulse at time 0 a

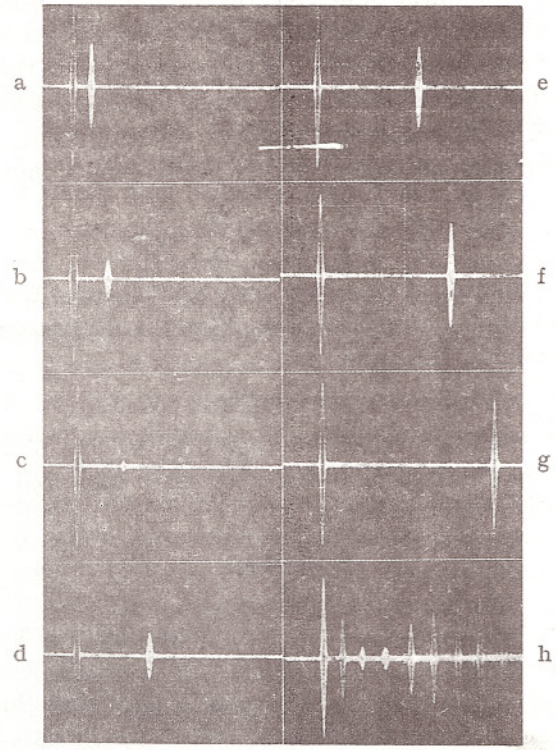

Fig. 26. 180° pulse signals of the cross-beam intensity for ^{199}Hg for different time intervals between the two succeeding pulses. In figure h, the preceding pictures have been superposed for tracing the τ_1 curve (COHEN-TANNOUDJI [1962a]).

second 180° pulse is applied at time t, the signal observed becomes

$$M_z(t) = M_z(0)(1-2e^{-t/\tau_1}).$$

Figures 26 a–g show two such successive pulse signals with different t intervals. Figure 26h shows a superposition of a number of such signals on the same plate.

The τ_1 curve can be traced by joining the tops of the signals.

3.3.2. *Relaxation of optically oriented alkali-atoms in pure vapours. Effects of wall coatings*

The first measurements of relaxation times in optically oriented *alkali-vapours* have been made in pyrex glass bulbs.

The relaxation times measured in pure vapours at low vapour-pressures are of the order of 10^{-4} s. Rough measurements showed that T_1 is proportional to the linear dimensions of the spherical or the cubic resonance cell. This is to be expected: At low vapour-pressure ($p < 10^{-3}$ mm Hg), where the mean free path is large compared to the dimensions of the vessel, the relaxation time T_1 can be identified with the 'mean time of flight' T_v of the atoms between two wall collisions.

In a vessel of volume V and of surface S, this time of flight is

$$T_v = \frac{N}{n} \cdot \frac{V}{S} = \frac{4}{\bar{v}} \cdot \frac{V}{S},$$

where N is the number of atoms per unit volume and n the mean number of wall collisions per unit surface. N and n are related by the formula of the kinetic theory:

$$n = \tfrac{1}{4} N\bar{v},$$

$\bar{v}$ is the mean thermal velocity $\bar{v} = \sqrt{(8kT/\pi m)} = \sqrt{(2.54\, RT/M)}$.

For a spherical bulb of diameter a, or for a cubic cell of length a, the ratio of volume to surface is

$$V/S = \tfrac{1}{6}a.$$

This gives $T_v = \frac{2}{3}\, a/\bar{v}$.

For ^{133}Cs at 300°K, $\bar{v} = 1.37 \times 10^4$ cm/s and for $a = 3$ cm, we find $T_v = 1.46 \times 10^{-4}$ s.

We conclude that at every collision on a glass wall the spin of an alkali atom is completely disoriented. Other experiments have shown that alkali atoms stick to glass surfaces, and in this case it is obvious that the relaxation time cannot be longer than the mean time of flight of the atoms.

In 1958 Dehmelt and coworkers (ROBINSON *et al.* [1958]) showed that much longer relaxation times could be obtained by covering the glass walls with special coatings of long-chain paraffines or of silicones (drifilm). This was confirmed by FRANZEN [1959] who measured for rubidium vapour in a paraffine-coated cell values of T_1 of the order of 10^{-1} s†.

The effect of different types of coatings on the longitudinal relaxation time T_1 of pure Rb isotopes has been systematically investigated by Mrs. BOUCHIAT [1962, 1963, 1964].

For obtaining reproducible results contamination of the bulb wall with metal deposite of rubidium must be carefully avoided. The rubidium metal is contained in a reservoir which communicates with the bulb through a thin capillary tube. In an other side-arm a barium getter serves to adsorb gas residues. Heating of the whole system to 65° C for several hours is necessary to obtain the normal saturation-vapour pressure in the bulb.

Mrs. Bouchiat used Franzen's method of transient signals in order to study the relaxation times. It can be shown that the change in light absorption is proportional to the electronic polarization $\langle S_z \rangle$ if the D_1 line alone (7947 Å) is used for pumping. (D_2 is suppressed by an interference filter.) All measurements have been made at 20° C.

The following results have been obtained by Mrs. Bouchiat: With the same coating T_1 is longer for ^{85}Rb than for ^{87}Rb. The ratio $T_1(85)/T_1(87)$ is about 2. For ^{87}Rb and paraffine or silicone coatings the relaxation times measured are 0.2 s in spherical bulbs of diameter 6 cm. For deuterated paraffines T_1 is about five times longer than for ordinary paraffines (1 s for ^{87}Rb and 2 s for ^{85}Rb).

This result shows that dipole–dipole interaction between the electron spin of the alkali atom and the nuclear spin of the coating is the dominant relaxation process (the nuclear magnetic moment of the proton is three times larger than the nuclear magnetic moment of the deuton).

The theory of dipole–dipole relaxation shows that the ratio $T_1(D)/T_1(H)$ should be 16 while the ratio found experimentally is only 5. This indicates that a second process (independant of the nuclear moments of the coating atoms) is contributing to the relaxation. This is probably the spin-orbit interaction studied by BERNHEIM [1962]. A study of T_1 at high steady fields indicates that the correlation time †† for

† For hydrogen atoms teflon coatings are very effective to preserve spin orientation (KLEPPNER *et al.* [1962]). Teflon coatings cannot be used with alkali vapours, they are chemically attacked by them.

†† For the definition of the correlation time τ_c *see* ABRAGAM [1961], p. 271.

dipole–dipole interaction is of the order of 10^{-10} s while it is much shorter ($\sim 10^{-12}$ s) for the second relaxation process. By changing the rubidium-vapour pressure Mrs. Bouchiat could show that the relaxation time for $\langle S_z \rangle$ is independent of this vapour pressure and that Rb–Rb collisions do not change the net $\langle S_z \rangle$ polarization. On the other hand the hyperfine populations (for $F = I + \frac{1}{2}$ state and $F = I - \frac{1}{2}$ state) are thermalized rapidly by Rb–Rb exchange collisions. The inverse hyperfine relaxation time $1/T_H$ is a linear function of the Rb-vapour pressure (Fig. 27) which leads to $1/T_{1H}$ for small Rb-vapour pressure.

The slope of the pressure dependence is the same for ^{85}Rb and for ^{87}Rb and does not depend on the coatings. From this slope the cross section for Rb–Rb exchange collisions is determined: $\sigma = 6 \times 10^{-14}$ cm^2. The transverse relaxation time T_2 has not been investigated by

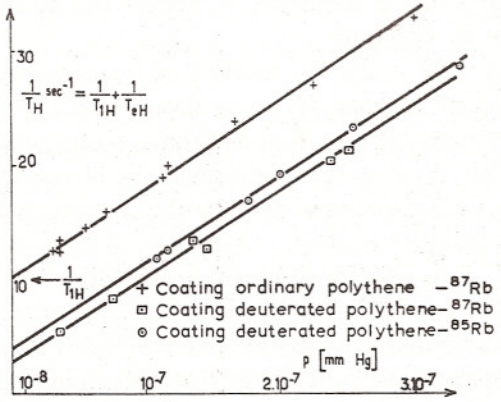

Fig. 27. Hyperfine relaxation rate of ^{87}Rb and ^{85}Rb in function of the Rb-vapour pressure. $1/T_{eH}$: relaxation rate by exchange collisions; $1/T_{1H}$: relaxation rate by wall collisions (different coatings) (BOUCHIAT and BROSSEL [1963]).

Mrs. Bouchiat. Qualitative measurements show that T_2 is roughly identical to T_1. Collisions of alkali atoms on coatings do not perturb the phase of the wave function. With coatings in pure vapours, very narrow resonance signals are obtained for Zeeman transitions ($\Delta\nu$ of a few c/s).

We may note that at low vapour pressure the effect of field inhomogeneity is suppressed by motion narrowing, the 'flying atom' seeing only the mean field-value inside the bulb.

Using Franzen's method, Cagnac has studied the relaxation time T_1 for nuclear orientation of the odd mercury isotopes ^{199}Hg and ^{201}Hg in fused silica cubic cells (CAGNAC [1960]).

At room temperature, T_1 is of the order of 3 to 5 s for ^{199}Hg. About 10^4 wall collisions are necessary to disorient the nuclear spin. To obtain this long relaxation time, the atoms of the vapour must be prevented to touch the mercury drop.

This fact results from a comparison of experiments in two cells a and b (Fig. 28). In cell a where the atoms can reach easily the drop, T_1 is shorter than in cell b where the drop is in a side-reservoir separated from the mean cell by a capillary.

Relaxation on the drop can be completely avoided by sealing off the capillary and by working on 'dry mercury vapour'. Doing this Cagnac studied the effect of a temperature change on the T_1 of dry mercury

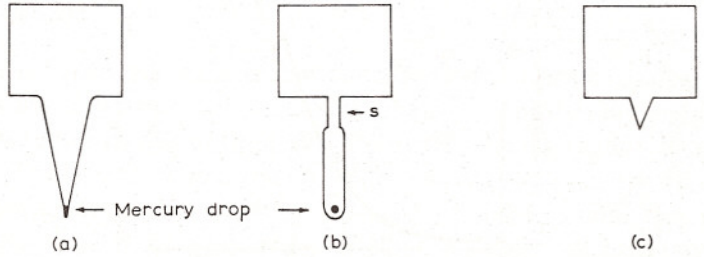

Fig. 28. Different shapes of resonance cells, a) large reservoir opening, b) reservoir with capillary s, c) scaled-off reservoir (dry mercury vapour).

vapour ^{199}Hg, by heating the cell in a hot air stream up to 350° C.

Figure 29 shows the result: T_1 grows rapidly with growing temperature and reaches 120 s at 300° C.

The study of T_1 as a function of the steady magnetic field value H_0 shows that the correlation time at room temperature is of the order of 10^{-6} s.

As the time of flight in the cell is of the order of 10^{-4} s, this correlation time must be related to the 'dwelling time' of the mercury atoms on the silica wall. The mean dwelling-time at room temperature must be at least 10^{-6} s. If the atoms of mercury would 'rebound' on the surface on the wall, the time of contact with the wall would be of the order of

$$t = 1\text{Å}/\bar{v} = 10^{-8}\text{cm}/10^4\ \text{cm}^{-1} = 10^{-12}\ \text{s}.$$

Cagnac's results show conclusively that the atoms are not rebounding, but are adsorbed at the wall. The mean time of adsorption becomes shorter with increasing temperature.

Relaxation occurs during this adsorption time through interaction of the nuclear spin with the wall atoms. For the ^{199}Hg nuclei of spin $i = \frac{1}{2}$ this interaction is of magnetic nature.

For ^{201}Hg the measurements show that T_1 depends also on the temperature, but that at each temperature $T_1(201)$ is about sixty times shorter than $T_1(199)$. ^{201}Hg has a nuclear spin $i = \frac{3}{2}$ and possesses an

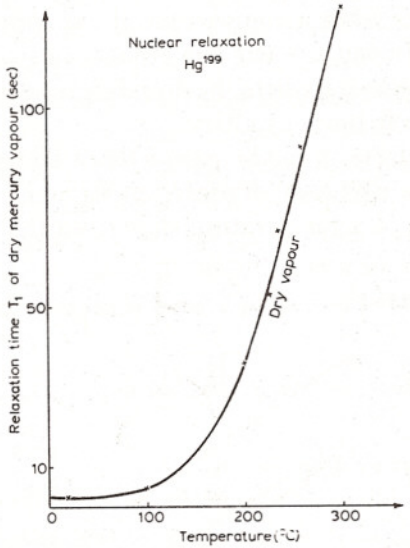

Fig. 29. Relaxation time T_1 of dry mercury vapour as function of the temperature of the fused silica walls (centigrade-scale) (CAGNAC [1960]).

electric nuclear quadrupole-moment. The strong relaxation of this nucleus must be attributed to an interaction of this quadrupole moment with electric-field gradients on the wall.

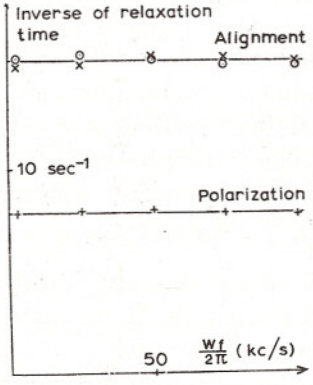

Fig. 30. Measurement of the relaxation rate of ^{201}Hg. Upper curve: results for aligned nuclei; lower curve: results for polarized nuclei (COHEN-TANNOUDJI [1963]).

The theory of this interaction has been developed by COHEN-TANNOUDJI [1963], who showed that relaxation should be two times more rapid for alignment than for polarization. This prediction has been checked experimentally (Fig. 30).

By different methods (width of the resonance lines, cross-beam techniques) T_2 has been measured for ^{199}Hg and for ^{201}Hg. It is of the same order of magnitude as T_1 but definitely smaller (for example for ^{199}Hg at room temperature $T_1 = 3$s and $T_2 = 1$s).

3.3.3. *Relaxation of alkali atoms in presence of diamagnetic gases (buffer gases)*

Early experiments showed that the addition of foreign diamagnetic gases to alkali vapours in glass cells enhanced considerably the magnetic-resonance signals of the alkali atoms (MARGERIE [1955], BENDER [1956], HARTMANN *et al.* [1958]). Collisions of alkali atoms with gas molecules prevent the optically oriented atoms to reach the walls where they lose their orientation. If the gas density is high enough (1 mm Hg), the mean free path of the atoms becomes small. The motion of the atom inside the bulb instead of being a free flight from wall to wall, tends to become a slow diffusion process in a gas atmosphere, the diffusion velocity being inversely proportional to the gas density.

This buffer-gas effect (protection against wall collisions) was explained by BENDER [1956] who showed that S-state atoms (without orbital momentum) are insensitive to molecular collisions. (But as we have seen in § 2.1.1.2, these collisions disorient the excited P states and change the optical-pumping conditions.)

COHEN-TANNOUDJI [1957] showed that buffer-gas collisions do not affect the phase of the spin wave functions and that very narrow resonance lines result. All these results show that by addition of a buffer gas, the relaxation process can be considerably slowed down.

Changing systematically the buffer-gas pressure in rubidium vapour, FRANZEN [1959] showed that there exists for each buffer gas an optimum pressure for which T_1 is maximum. For higher pressures T_1 decreases again.

Similar results were obtained for sodium vapour (ANDERSON and RAMSAY [1963]). The results are summarized in Table 4 and illustrated by Fig. 31.

This behaviour shows that collisions with buffer-gas molecules are

finally relaxing, but that the cross section for spin disorientation is very small. It is the smaller, the smaller the polarizability of the buffer gas. Hydrogen and especially helium are most efficient to obtain very long relaxation times ($T_1 = 2$ s for He at atmospheric pressure).

From the curves which show T_1 as function of the buffer-gas pressure the cross section σ for spin disorientation can be calculated. It ranges from 10^{-20} cm² for xenon to 10^{-26} cm² for helium.

The theory of the disorientation effect by buffer-gas collisions has been developed by BERNHEIM [1962] and by HERMAN [1964].

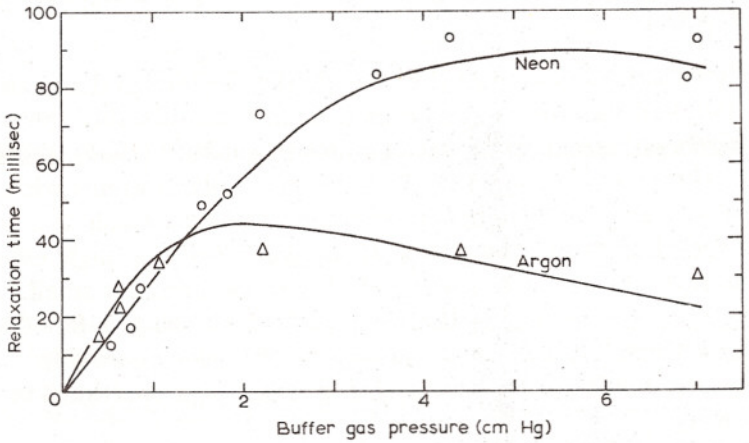

Fig. 31. Relaxation time T_1 of optically oriented vapour as a function of buffer-gas pressure (neon and argon) (FRANZEN [1959]).

As in the case of disorientation by wall coatings two interactions can be envisaged: the dipole–dipole interaction between electron spin and the nuclear spins of the buffer-gas molecules, and the spin-orbit interaction analysed by Bernheim.

BREWER [1962] has measured the disorientation cross-section of Rb atoms for H_2 and D_2. If dipole–dipole interaction would be predominant, H_2 with the stronger nuclear moment should be more efficient for disorientation than D_2. The cross sections measured indicate that this is not the case.

HERMAN [1964] has shown that the Bernheim interaction has the right magnitude, but that indirect dipole–dipole interaction produced by the Pauli exchange forces and envisaged by ADRIAN [1960] may contribute to the relaxation and may be at the origin of nuclear polarization by collision with oriented paramagnetic atoms.

Actually this question remains open. A comparison of σ for ^{3}He and ^{4}He (where dipole–dipole interaction is absent) would be of considerable interest.

MCNEAL [1964] has studied recently spin relaxation of optically pumped rubidium atoms, by adding to an atmosphere of nitrogen, at a pressure of 35 mm Hg and at a temperature of 55° C, small quantities of various strongly relaxing molecules, at a partial pressure of 10^{-3} to 10^{-2} mm Hg. The disorientation cross-section of molecular nitrogen is only 5.7×10^{-23} cm². The gases or vapours added to nitrogen are CO, $(CH_3)_2O$, NH_3 and C_6H_6. Their respective disorientation cross-sections are as follows:

$$\begin{aligned} &CO && \sigma = (1\pm0.5)\times10^{-22}\ \text{cm}^2\\ &(CH_3)_2O && \sigma = (3\pm1)\times10^{-18}\ \text{cm}^2\\ &NH_3 && \sigma = (8\pm2)\times10^{-18}\ \text{cm}^2\\ &C_6H_6 && \sigma = (7\pm1)\times10^{-19}\ \text{cm}^2. \end{aligned}$$

According to the author the very large cross-sections of $(CH_3)_2O$ and NH_3 are related to the strong electric dipole-moment of these molecules. The strong electric fields in the neighbourhood of these dipoles induce in the Rb atom a Stark-effect mixing to the S ground state excited P states. A strong disorientation of the electron spin results.

TABLE 4

Relaxation by buffer gases

Alkali atom	Buffer-gas	Optimum pressure	Max T_1	σ
Rb (FRANZEN [1959])	Ne	6 cm Hg	10^{-1} s	5.2×10^{-23} cm²
	Ar	2 cm Hg	4×10^{-2} s	3.7×10^{-22} cm²
	Kr	0.1 cm Hg	1.5×10^{-2} s	5.9×10^{-21} cm²
	Xe	0.05 cm Hg	1.2×10^{-2} s	1.3×10^{-20} cm²
Na (ANDERSON and RAMSEY [1963])	He	70 cm Hg	2 s	3×10^{-26} cm²
	Ne	10 cm Hg	0.5 s	1.8×10^{-24} cm²
Rb (BREWER [1963])	H_2			2.2×10^{-24} cm²
	D_2			4.3×10^{-25} cm²
Rb (MC NEAL [1964])	N_2			5.7×10^{-23} cm²

The high disorientation cross-section of benzene, whose molecule has no dipole moment, is attributed to a charge exchange between the Rb atom and the C_6H_6 molecule. This interpretation is supported by BREWER [1964]. He has shown that the charge exchange produces also an anomalously large shift of the hyperfine frequency of Rb towards lower frequencies. The shift measured by Brewer is proportional to the benzene density and amounts to $\Delta\nu = -136$ c/s for a partial pressure of benzene equal to 10^{-3} cm Hg. This value is considerably larger than the shifts observed in normal buffer gases.

We have seen that long relaxation times, and as a consequence high degrees of orientation, can be obtained either by suitable wall coatings or by suitable buffer gases. The longest relaxation times can be obtained by using together both a coating and a buffer gas. For example, we can use a deuterated paraffine-coating and helium gas at a pressure of 1 to 10 cm Hg.

The answer to the question: 'What is the best choice? Coating or buffer gas?' depends on the aim of the study, especially if very narrow resonance-lines are desired. For low-frequency Zeeman lines for which Doppler broadening is negligible, coatings are preferable to buffer gas, the field inhomogeneity inside the cell being reduced in this case by motion narrowing. For high-frequency hyperfine intervals, where Doppler broadening $(\Delta\nu/\nu) \sim 10^{-6}$ is important, the line-breadth can be reduced by the reduction of the mean free path in buffer gases (DICKE [1953]). This is particularly interesting for field-independent frequencies ($0 \leftrightarrow 0$ hyperfine transition).

However, the frequency of the line is shifted by the buffer gas collisions.

At high buffer gas pressures, the atoms diffuse slowly. In this case, field inhomogeneities inside the bulb will cause for field-dependent frequencies broadening of the lines. Buffer gas has another disadvantage in the case of strong absorption of the pumping light: the degree of orientation will, in this case, depend on the distance of the atoms to the entrance window of the light. The degree of orientation is not uniform inside the bulb, and the quantitative interpretation of detection signals is a complicated problem.

3.4. INTERACTIONS BETWEEN THE ATOM AND THE ELECTROMAGNETIC FIELD

3.4.1. *Effects of light on atomic-energy levels*

3.4.1.1. Quantum theory of the optical-pumping cycle

We will now see how optical pumping has made it possible to study

very small effects related to the interaction between the atom and the electromagnetic field. These effects have been predicted from a quantum theory of the optical-pumping cycle (BARRAT and COHEN-TANNOUDJI [1961], COHEN-TANNOUDJI [1962a]). They have been observed experimentally (COHEN-TANNOUDJI [1961a, b-1962a], ARDITI and CARVER [1961], SHEARER [1962]).

Let us just remark that the necessity of a quantum theory of the optical-pumping cycle is clearly demonstrated by several experimental facts. So, in order to give a quantitative interpretation of the experiments described in § 2.4, we must know the time evolution under the effect of optical pumping of the non-diagonal elements of the density matrix, and also the expression connecting the optical-detection signals to these non-diagonal elements. Another example: one observes experimentally that the stronger is the light intensity of the pumping beam, the broader are the magnetic-resonance curves in the ground state. This is easy to understand: the absorption of an optical photon stops the coherent action of the radiofrequency field. So, the light beam, which in optical-pumping experiments may be considered in a certain manner as a measuring instrument since it permits to orient the atoms and at the same time to detect this orientation, perturbs the physical system which it allows to study. We are thus led to the problem of evaluating quantitatively this perturbation and of seeing if it amounts only to a broadening of atomic-energy levels. We will see later on that there is also a shift of the energy levels.

In this article, we will not describe in detail the quantum theory of optical pumping. We will just give a brief outline of the theory, a physical interpretation of the new effects predicted, and a rapid description of the experiments which have confirmed the existence of such effects.

The density-matrix formalism is used for the description of the ensemble of atoms, the quantum theory of radiation for the description of the light beam. One starts from the Schrödinger equation which gives the time evolution of the ensemble atoms plus radiation field and one solves this equation by a second-order perturbation treatment. Admitting certain conditions which are always fulfilled in practical cases (this would not be the case with a laser as the light source) and which are: weak density of photons, large line-width of the pumping light, great indetermination on the phase of the light wave, one derives the following results:

a. The time evolution of the density matrix σ which represents the

ensemble of atoms, $(\mathrm{d}/\mathrm{d}t)\sigma$ may be written as a sum of three terms:

$$\frac{\mathrm{d}}{\mathrm{d}t}\sigma = \frac{\mathrm{d}^{(1)}}{\mathrm{d}t}\sigma + \frac{\mathrm{d}^{(2)}}{\mathrm{d}t}\sigma + \frac{\mathrm{d}^{(3)}}{\mathrm{d}t}\sigma.$$

The first term represents the effect of optical excitation by the light beam; the second term, the effect of spontaneous emission, the third term, the effect of processes other than the interaction between the atom and the radiation field (Larmor precession, effect of a radiofrequency field, relaxation . . .). The explicit expression of the two first terms is given. One finds them in all optical-pumping experiments. From one experiment to another, only the third term changes.

b. Theory gives also the exact expression of the optical-detection signals. The quantity of light $L_A(\boldsymbol{e}_{\lambda_0})$ of polarization $\boldsymbol{e}_{\lambda_0}$, absorbed per unit time by the vapour may be written as a linear combination of the elements of the density matrix in the ground state; the quantity of light $L_F(\boldsymbol{e}_\lambda)$ of polarization $\boldsymbol{e}_\lambda$, reemitted by the vapour, may be written as a linear combination of the elements of the density matrix in the excited state.

It is therefore possible to carry out the calculation appropriate to an optical-pumping experiment in a systematic way. One has just to solve the equation which gives $(\mathrm{d}/\mathrm{d}t)\sigma$, in order to obtain σ for all values of t. One then deduces from σ the optical signals, L_A and L_F which makes it possible to interpret completely the experimental results.

With regard to the populations of the different energy sublevels, the previous theory gives the usual well-known results. It justifies rigorously the intuitive physical picture of the optical-pumping cycle. Some new results appear in connection with the study of the non-diagonal elements of the density matrix. We will now study their physical interpretation.

3.4.1.2. Shift and broadening of atomic-energy levels due to optical excitation

The most important result of the theory is the following: Atomic levels in the ground state are broadened and shifted by irradiation with resonance radiation. This appears as a broadening and as a shift of the magnetic-resonance curves in the ground state.

Two important parameters describe this effect: the finite life-time, T_P and the displacement, $\Delta E'$, of the ground-state sublevels due to optical excitation. In Figs. 32a, b, we have represented on the one hand, the spectral distribution of the light intensity, $u(k)$, centered at frequency k_1 and having a width Δ and on the other hand, the atomic absorption (Fig. 32a) and dispersion (Fig. 32b) curves centered at the resonant optical frequency k_0 and having a width Γ (Γ is the natural width of the excited state; we assume that $\Delta \gg \Gamma$). The theoretical expression giving $1/T_P$ (and $\Delta E'$) is equal to the integral from $-\infty$ to $+\infty$ of the product: $u(k)$ times the atomic absorption (and dispersion) curve. $1/T_P$ and $\Delta E'$ are obviously proportional to the light intensity. It is easy to deduce from Figs. 32a, b the variation of $1/T_P$ and $\Delta E'$ with $k_1 - k_0$. Since Δ is large compared to Γ, $1/T_P$ is proportional to $u(k_0)$.

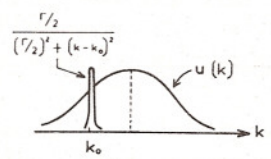

Fig. 32a. Method of evaluating the absorption shape integral of $1/T_P$.

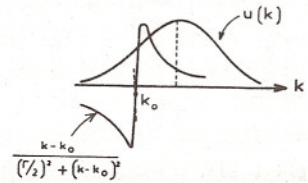

Fig. 32b. Method of evaluating the dispersion shape integral of $\Delta E'$ (COHEN-TANNOUDJI [1962a]).

$1/T_P$ has therefore the same variation as $u(k)$ and has maximum when $k_1 = k_0$. On the other hand, $\Delta E'$ is zero, for reason of symmetry, when $k_1 = k_0$. It increases with $k_1 - k_0$ until a maximum is reached. This maximum is of the same order of magnitude as the maximum of $1/T_P$ and occurs when $k_1 - k_0$ is of the order of Δ. Then $\Delta E'$ decreases, but much more slowly than $1/T_P$ so that, for sufficiently high values of $k_1 - k_0$, $1/T_P$ is completely negligible whilst $\Delta E'$ is still appreciable. (An absorption curve decreases as $(k - k_0)^{-2}$, but a dispersion curve decreases only as $(k - k_0)^{-1}$.)

This difference of behaviour between $1/T_P$ and $\Delta E'$ suggests that one ascribes the physical effects associated with these quantities to two different types of transitions. When there are in the light beam photons having an energy equal to the energy of the atomic transition, these photons may be actually absorbed by the atom. The corresponding transitions satisfy the principle of conservation of energy: these are 'real transitions'. They give to the ground state a finite life-time as they make the atom leave this ground state. On the other hand, if the energy of the photon is not equal to k_0, a real absorption cannot take place, for energy would not be conserved. The atom may however absorb virtually the photon provided this virtual absorption lasts a sufficiently short time (less than $\hbar/(k_1 - k_0)$ because of the fourth

uncertainty relation). The effect of this 'virtual transition' is to bring back into the wave function of the ground state a small part of the wave function of the excited state, and so to modify slightly the energy of the ground state.

What we have just described is the effect of real and virtual transitions on the atomic system. It is interesting to remark that these two types of transitions have also an effect on the light beam and that this effect has been known for a long time. After a real transition a photon has disappeared from the light beam: this is the *absorption* phenomenon. During a virtual transition, the propagation of the photon is stopped for a very short time: the photon is not absorbed but its velocity is slightly changed. This is the phenomenon of *anomalous dispersion*.

Another point must be emphasized: the radiative effects we have described are related to the optical-excitation process. Similar effects exist also for the spontaneous emission process and are well known: an excited atom may undergo a real transition, jumping to a lower level and emitting spontaneously a photon. This explains the radiative life-time of the excited state and the *natural width* of this state. While the atom is in the excited state, virtual emissions and reabsorptions of photons may also occur. This gives a self energy to the excited state and is responsible for the 'Lamb shift' (LAMB [1951]). There is however an important difference between the two effects: spontaneous emission is an isotropic process: All Zeeman sublevels of the excited state have the same natural width and the same self-energy. This is not the case for the optical excitation process. By choosing a convenient polarization for the light beam, it is possible to broaden and to displace differently the various sublevels of the ground state. This is very important for the experimental observation of $\Delta E'$. With the usual light intensities $\Delta E'$ is very small as compared to Γ. It is hopeless to attempt to observe the displacement $\Delta E'$ on the optical lines emitted by the atom, as these lines have a spectral width at least equal to Γ. On the other hand, the magnetic-resonance curves in the ground state are considerably narrower, but they are shifted by the light irradiation only if the different Zeeman sublevels are shifted differently.

The experimental observations of the displacement $\Delta E'$ associated with the virtual transitions have been made on ^{199}Hg which has only two Zeeman sublevels in the ground state (COHEN-TANNOUDJI [1961b]). The experiment is done in two steps. In a first step, one repeats Cagnac's experiment (CAGNAC [1960]): One optically pumps the vapour

with a light beam, one performs the magnetic resonance and one measures with a very high precision the energy difference between the two Zeeman sublevels. In a second step, one irradiates the atoms with a second light beam which is propagated in a direction opposite to the first one and one observes whether this second light beam perturbs the magnetic-resonance curve. The experimental conditions are evidently choosen in such a manner that the displacement $\Delta E'$ associated with the second beam has the greatest possible value: In order to obtain $k_1 \neq k_0$, the lamp producing the second light beam is filled with an isotope other than ^{199}Hg. (One chooses in fact ^{201}Hg, because one hyperfine component of this element is about one Doppler-width distant from the component $\frac{1}{2}$ of ^{199}Hg, which according to Fig. 32b, corresponds to the optimum value for $\Delta E'$.) In order to eliminate all the *real* transitions which can be excited by the wings of the ^{201}Hg spectral line, a ^{199}Hg filter is added between the light source and the resonance cell. This filter absorbs all the resonant wave-lengths in the spectrum of the second beam which, therefore, excites only pure virtual transitions in the cell. This light beam is either right or left circularly polarized. One sees immediately from the transition probabilities of the component $\frac{1}{2}$ of ^{199}Hg that, in the first case, only the sublevel $|-\frac{1}{2}\rangle$ is shifted, whereas in the second case, only the sublevel $|+\frac{1}{2}\rangle$ is shifted (with the same sign and with the same quantity) (Fig. 33).

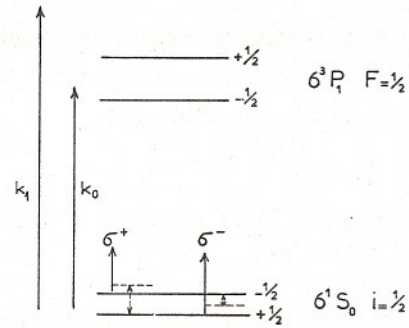

Fig. 33. Scheme for ^{199}Hg (a hyperfine component $i = \frac{1}{2} \rightarrow F = \frac{1}{2}$ of 2537 Å), showing the shift of ground-state Zeeman-levels produced by virtual transitions of frequency $k_1 > k_0$ (COHEN-TANNOUDJI [1962a]).

The experimental results, represented in Fig. 34 agree completely with the theoretical predictions. The presence of the second beam shifts the magnetic-resonance curve (there is no broadening as the

transitions are virtual). Changing the second light beam from σ^+ to σ^- changes the sign of the shift. This shift is very small: 0.5 c/s for a magnetic-resonance frequency of 5 000 c/s. The variation of $\Delta E'$ with $k_1 - k_0$ has been also observed by varying k_1 in a magnetic-scanning experiment. The results, represented in Fig. 35, clearly show that $\Delta E'$ varies with $k_1 - k_0$ like a dispersion curve.

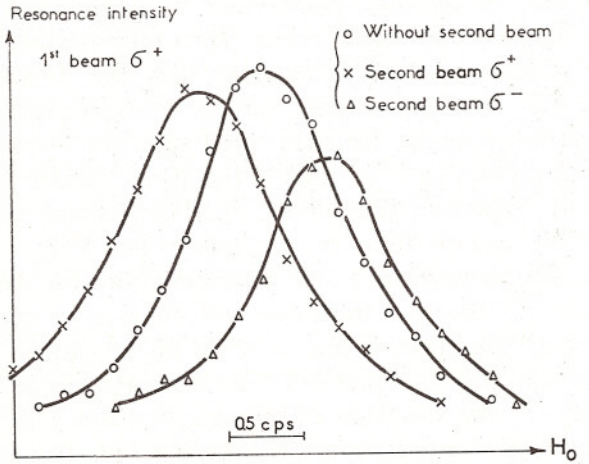

Fig. 34. Experimental proof of the shift of the nuclear magnetic-resonance line center of ^{199}Hg, produced by virtual transitions (at constant frequency and variable H_0 field) (COHEN-TANNOUDJI [1962a]).

Light shifts of magnetic-resonance curves have been also observed by other physicists. ARDITI and CARVER [1961] mention the existence of light shifts for the $0 \leftrightarrow 0$ hyperfine transition in the ground state of alkali atoms (this transition is looked at in optically pumped atomic clocks). SHEARER [1962] has also observed light shifts of the magnetic-resonance curves in the 2^3S state of He.

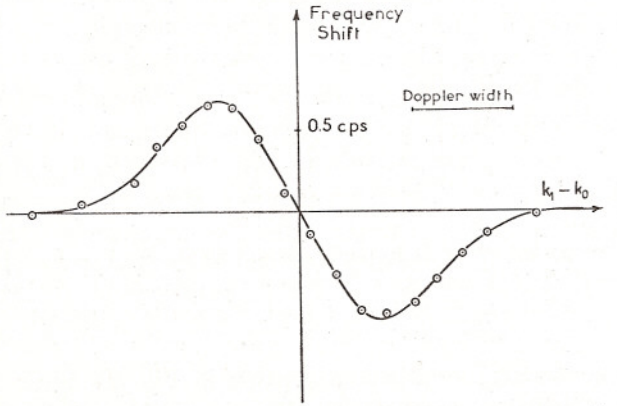

Fig. 35. Frequency shift produced by virtual transitions as a function of $k_1 - k_0$ (COHEN-TANNOUDJI [1962a]).

3.4.1.3. Carry over of coherence along the optical-pumping cycle

Another important effect predicted by the theory is the possibility of a partial conservation of coherence during the optical-pumping cycle. In more physical terms, the transverse angular momentum of an atom keeps, during the different steps of the optical-pumping cycle, a certain memory of the direction which it had at the beginning of the cycle. This has some important consequences which we will now review.

a. If there is some hertzian coherence in the ground state, optical excitation transfers permanently a certain fraction of this coherence to the excited state. There appears therefore, in the excited state, a macroscopic transverse magnetization $\langle \boldsymbol{M}_\perp \rangle_e$ which undergoes a *forced motion* at the Larmor frequency ν_f of the ground state. But the own frequency of $\langle \boldsymbol{M}_\perp \rangle_e$, which is the Larmor frequency ν_e of the excited state, is, in general, different from ν_f; the motion of $\langle \boldsymbol{M}_\perp \rangle_e$ is, on the other hand, damped with a time constant $\tau = 1/\Gamma$ which is the radiative life-time of the excited state. The forced motion of $\langle \boldsymbol{M}_\perp \rangle_e$ at frequency ν_f is, therefore, possible only if $|\nu_e - \nu_f| \lesssim \Gamma$, i.e. if the field H_0 is sufficiently small; in addition, a phase difference is produced between $\langle \boldsymbol{M} \rangle_e$ and $\langle \boldsymbol{M} \rangle_f$ which comes from the difference between ν_e and ν_f. When H_0 is increased, the amplitude of $\langle \boldsymbol{M}_\perp \rangle_e$ decreases and tends to zero, the phase difference between $\langle \boldsymbol{M}_\perp \rangle_e$ and $\langle \boldsymbol{M}_\perp \rangle_f$ tends to a limit $\frac{1}{2}\pi$.

This behaviour of $\langle \boldsymbol{M}_\perp \rangle_e$ has been observed experimentally by studying the modulation of the fluorescent light at the frequency ν_f of the ground state (COHEN-TANNOUDJI [1962a]). (It may be shown that this modulation reflects directly the motion of $\langle \boldsymbol{M}_\perp \rangle_e$.)

b. Spontaneous emission gives back to the ground state some fraction of the coherence which has been pulled out of this state by optical excitation: a certain fraction of $\langle \boldsymbol{M}_\perp \rangle_e$ returns to $\langle \boldsymbol{M}_\perp \rangle_f$ by spontaneous emission. The above analysis on $\langle \boldsymbol{M}_\perp \rangle_e$ shows that this restitution of coherence is important only in sufficiently weak fields ($|\nu_e - \nu_f| \lesssim \Gamma$) and occurs with a phase difference. More quantitatively, if we call $\sigma_{\frac{1}{2},-\frac{1}{2}}$ the non-diagonal element of the density matrix in the ground state, we have:

$$\frac{\mathrm{d}}{\mathrm{d}t}\sigma_{\frac{1}{2},-\frac{1}{2}} = -\frac{1}{T_P'}\sigma_{\frac{1}{2},-\frac{1}{2}} + \left(\frac{1}{T_P''} - 2\pi i\varepsilon''\right)\sigma_{\frac{1}{2},-\frac{1}{2}} - 2\pi i\nu_f\sigma_{\frac{1}{2},-\frac{1}{2}}$$

with

$$\frac{1}{T_P'} = \frac{A}{T_P}, \qquad \frac{1}{T_P''} = \frac{B}{T_P}\frac{\Gamma^2}{\Gamma^2+4\pi^2(\nu_e-\nu_f)^2}, \qquad \varepsilon'' = \frac{B}{T_P}\frac{\Gamma(\nu_e-\nu_f)}{\Gamma^2+4\pi^2(\nu_e-\nu_f)^2}$$

(A and B are dimensionless coefficients which depend on the polarization of the light beam).

The first term of the equation represents the disappearance of coherence from the ground state due to optical excitation, the second term, the restitution of coherence by spontaneous emission. The imaginary part of this term comes from the phase difference between $\langle M_\perp\rangle_e$ and $\langle M_\perp\rangle_f$. $1/T_P''$ and ε'' depend on the magnetic field through $\nu_e-\nu_f$, which is clearly understandable from the above considerations about $\langle M_\perp\rangle_e$. Finally the third term of the equation represents the proper evolution of $\sigma_{\frac{1}{2},-\frac{1}{2}}$ in the ground state (Larmor precession).

Rearranging the terms of the equation, it appears first that optical pumping changes the frequency of the Larmor precession in the ground state from ν_f to $\nu_f+\varepsilon''$. The optical pumping cycle brings back, therefore, in the g factor of the ground state a small part of the g factor of the excited state. This leads to a second type of shift of the magnetic-resonance curves in the ground state, produced by light irradia-

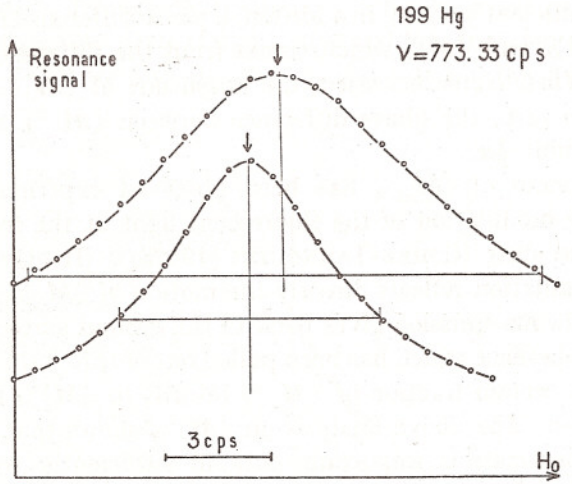

Fig. 36. The two effects of light relaxation by the cross beam (real transitions): broadening and shift of the resonance curve for high light intensity (COHEN-TANNOUDJI [1962a]).

tion. This shift is produced by real transitions, and not by virtual transitions as it was the case for $\Delta E'$ (ε'' is proportional to $1/T_P$). For the experimental observation of this effect, two light beams are used (COHEN-TANNOUDJI [1961d]). To isolate this second type of shift, the characteristics of the second beam have to be choosen in such a way that $\Delta E'$ is zero. Figure 36 shows an experimental result. The two curves of this figure correspond to different light intensities for the second beam ($\frac{1}{5}\mathscr{I}$ for the curve to the left, $\mathscr{I}$ for the curve to the right). The shift of the magnetic-resonance curve, produced by the second beam and proportional to its intensity, appears clearly. The curve is also broadened. (The second beam induces real transitions and shortens the life-time of the ground state.)

The variation of ε'' with H_0 has also been studied experimentally (Fig. 37). The curve is drawn according to the theoretical expression, the points are experimental.

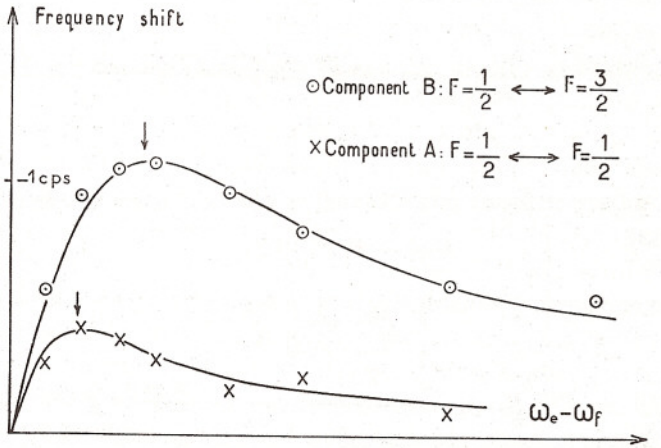

Fig. 37. Frequency shift produced by real transitions: A = hyperfine component and B = hyperfine component of 2537 Å, ^{199}Hg (Cohen-TANNOUDJI [1962a]).

One deduces from the above expression that $\sigma_{\frac{1}{2},-\frac{1}{2}}$ is damped by the light irradiation with a time constant τ_P, such that

$$\frac{1}{\tau_P} = \frac{1}{T_P'} - \frac{1}{T_P''}.$$

Unlike T_P', T_P'' depends on H_0. One readily sees that τ_P is longer in weak fields than in strong fields.

In order to measure τ_P, one makes use of the free-precession signals described in § 2.4.2. The whole damping of $\langle \boldsymbol{M}_\perp \rangle_f$ (i.e. $\sigma_{\frac{1}{2},-\frac{1}{2}}$) is due, on the one hand, to the thermal relaxation (time constant T_2) and on the other hand to optical pumping ('optical relaxation' with a time constant τ_P). The whole time constant τ_2 which appears in Fig. 24, is therefore such that

$$\frac{1}{\tau_2} = \frac{1}{T_2} + \frac{1}{\tau_P}.$$

As $1/\tau_P$ is proportional to the light intensity $\mathcal{I}$ one can measure $1/\tau_2$ for different values of the light intensity $\mathcal{I}$ of the second beam, and then deduce by extrapolation T_2 and τ_P. The variation of $1/\tau_P$ with H_0 (Fig. 38) agrees completely with the theoretical predictions (curves are based on theory, the points represent results of experiments).

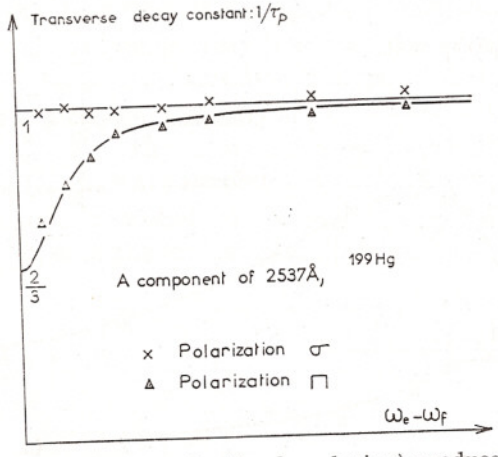

Fig. 38. Transverse relaxation rate (line broadening) produced by real optical transitions, as a function of $\omega_e - \omega_f$ (COHEN-TANNOUDJI [1962a]).

So, we see that coherence as well as the populations is carried over along the optical-pumping cycle. This carry over depends on H_0 and has some important physical consequences.

Before ending this section, we would like to mention that LEHMANN [1964b] has extended the quantum theory of optical pumping to the case where the hyperfine structure in the excited state is of the same order of magnitude as the natural width of this level. Such a situation occurs for the odd isotopes of cadmium and it affects considerably the mechanism of nuclear orientation by optical pumping. Some new effects, related to the existence of hyperfine coherence in the excited state, are predicted by the theory and are being observed. BOUCHIAT [1964] has extended the quantum theory of optical pumping to the alkali atoms which have a hyperfine structure in the ground state.

3.4.2. *Multiple quantum transitions*

One of the first studies of multiple-quantum-transitions has been done on an optically pumped alkali-vapour. This is another example of a problem related to the interaction between the atom and the electromagnetic field where optical-pumping techniques have given important contributions. (The electromagnetic field involved here belongs to a radiofrequency wave and not to a light wave.)

Let us call m_F the Zeeman sublevels of the ground state of an alkali atom. Owing to I–J decoupling, these sublevels are not equidistant. By increasing the intensity of the radiofrequency field, BROSSEL *et al.* [1953, 1954] have observed, between the normal resonances, $\Delta m_F = 1$, multiple resonances, $\Delta m_F > 1$ involving several electromagnetic quanta. These quanta have all the same polarization (circular quanta of angular momentum $+1$ with respect to H_0). During a multiple transition, the number of quanta is such that energy and total angular momentum are conserved. Theoretical studies of these transitions have been made by BESSET *et al.* [1954], WINTER [1955a, b, 1959, 1962], SALWEN [1955, 1956] and HACK [1956]. Winter has also predicted and observed other types of multiple transitions involving simultaneously several quanta of different energies and different angular momenta: we will not analyse Winter's work here. We will only mention that it has permitted to explain all the characteristics of these transitions: variation of the intensity and the width of the resonance with the radiofrequency power, radiative displacements etc.

Let us finally mention that, owing to the strong intensities of light produced by lasers, it has been recently possible to observe the same phenomena in the optical range (ABELLA [1962]).

3.5. SPIN EXCHANGE COLLISIONS

Only a small number of atomic species (alkali atoms, mercury nuclei, ^{3}He) can be oriented directly by optical pumping with resonance radiation in a spectral range where polarization techniques are available (visible spectrum, near infrared and near ultraviolet). For other atoms,

especially those whose resonance radiation is in the far UV, direct optical pumping is not possible.

These species can be oriented indirectly through spin-exchange collisions. We have already mentioned the principle of this method (see § 2.1.1.5) and have shown that by these means it was possible to measure (or remeasure) the hyperfine structure of hydrogen, deuterium and tritium (ANDERSON *et al.* [1960], PIPKIN and LAMBERT [1962]), nitrogen ^{14}N and ^{15}N (HOLLOWAY *et al.* [1962], LAMBERT and PIPKIN [1963]), phosphorus ^{31}P (LAMBERT and PIPKIN [1962]) and the gyromagnetic factor of silver and of free electrons (DEHMELT [1958], HOBART [1962], BALLING *et al.* [1964]).

In a mixture of two alkali vapours, e.g. Rb and Cs, one species can be oriented by pumping and detecting with the resonance radiation of the other species. In this way, resonances of isotopes present in small concentration can be detected (ALEKSANDROV and KHODOVOI [1962]).

Spin exchange is a strong interaction. The spin-exchange collision cross-sections lie in the range of 10^{-14} cm^2. Table 5 gives a review on different values actually measured.

TABLE 5

Spin exchange cross-sections measured by optical-pumping methods

Atoms	Q in units of 10^{-14} cm^2	Author
Na+electron	> 2.3	DEHMELT [1958]
Na+^{85}Rb	~ 2	NOVICK and PETERS [1958]
Na+K	~ 5	FRANKEN *et al.* [1958]
^{87}Rb+^{87}Rb	4–7	CARVER [1959]
Na+Na	6	ANDERSON and RAMSEY [1961]
^{85}Rb+^{87}Rb	1.7 ± 0.2	JARRETT [1962]
^{85}Rb+^{85}Rb ^{87}Rb+^{87}Rb ^{87}Rb+^{85}Rb	6	BOUCHIAT and BROSSEL [1963]

The results of the measurements depend essentially on the observable which is detected.

The theoretical evaluation of spin-exchange cross-sections is a difficult problem, because of our imperfect knowledge of the interatomic forces on which the exchange process depends.

In a very rough way, we can say that when two paramagnetic atoms collide, electrons between them are exchanged, each electron keeping its proper spin orientation. For identical atoms without nuclear spin colliding, such an exchange process is unobservable. If both atoms or only one have nuclear spin, the coupling between nuclear and electron spin is interrupted during the exchange process. This process is a 'sudden' process which means that the time of exchange is small compared to the different precession periods of the atom (precession of $\boldsymbol{F}$ around an external field, precession of $\boldsymbol{J}$ and $\boldsymbol{I}$ around F). The nuclear spin of each atom keeps its instantaneous orientation during the exchange process and rearranges its coupling with the new electron after the exchange has taken place.

During the exchange process itself 'nuclear orientation is conserved'. It is changed subsequently by the process of recoupling with the electron.

We may compare this to the Franck–Condon principle according to which in a molecule 'nuclear position is conserved' in an electronic transition.

Using this rough model it can be shown that the average value of the total polarization of a collection of atoms $\langle F_z \rangle - \langle S_z \rangle + \langle I_z \rangle$ is conserved by spin exchange. The effect of exchange results in a rapid thermalization between hyperfine levels. A theoretical study of hyperfine relaxation by hydrogen–hydrogen collisions has been made by WITTKE and DICKE [1954]. It has been extended to collisions between two identical or unidentical alkali atoms by Mrs. GROSSETÊTE [1964a]. The experimental verification of predicted results has been made on the Rb-Cs couple and is continued on Rb–Rb collisions (GROSSETÊTE [1964b]). The theoretical calculation of the absolute values of spin-exchange cross-sections for H–H collisions has also been recently discussed by GLASSGOLD [1963, 1964].

Exchange collisions produce a shift of the resonance frequency. This shift has been studied theoretically and experimentally by BALLING *et al.* [1964] for the resonance frequency of free electrons oriented by optically pumped Rb-vapour. The shift which depends on the sign of the Rb polarization is found experimentally to be of the order of 2 % of the line-width. This shift is certainly smaller in the case of exchange collisions of two alkali atoms.

A special case of spin exchange collisions is the *'metastability exchange'*. If a ground-state atom and a metastable atom of the same species collide, the excitation energy can be exchanged between the

two colliding atoms, the spin orientation of the electrons being conserved in this process. In absence of nuclear spin, this exchange process is unobservable.

In case of nuclear spin, the spin orientation of each atom is conserved. If in one of the two states, e.g. in the metastable state, the nuclear spin has been previously oriented, this orientation is transferred to the other state. By this efficient method, nuclear orientation produced optically in the 2^3S_1 metastable state of ^{3}He can be transferred to the ground state 2^1S_0 (COLEGROVE *et al.*[1963]). A nuclear degree of polarization of 40 % has been obtained by this method in ^{3}He gas at 1 mm pressure.

§ 4. Practical Applications of Optical Pumping

Optical-pumping techniques are applied in two types of instruments:

– *magnetometers* for measuring small magnetic fields, especially the earth field at the surface of the earth and at high altitude, and

– *frequency standards* (*atomic clocks*) designed to keep and to reproduce a reference frequency.

The resonance lines obtained in optical-pumping devices are very narrow, of the order of some c/s. With a good signal to noise ratio the center of the line can be determined with an accuracy of 10^{-1} c/s or even better.

As a result of this high accuracy precision measurements can be made in both cases.

4.1. MAGNETOMETERS

For field measurements the low-frequency Zeeman transitions $\Delta F = 0$, $\Delta m = 1$ of alkali atoms or the Zeeman transition $\Delta m = 1$ of the metastable state 2^3S_1 of ^{4}He are used. In weak fields the Zeeman-resonance frequency is a linear function of the field and its value is given by

$$\nu = \frac{2\mu_B}{h} H \qquad \text{for helium}$$

and by

$$\nu_{F_1} = \frac{\mu_B H}{h}\left[\frac{g_j}{2i+1} + \frac{2i}{2i+1} g_i\right] \qquad \text{for } F_1 = i+\tfrac{1}{2}$$

$$\nu_{F_2} = \frac{\mu_B H}{h}\left[\frac{g_j}{2i+1} - \frac{2(i+1)}{2i+1} g_i\right] \qquad \text{for } F_2 = i-\tfrac{1}{2}$$

for the two hyperfine states of the ground state of alkali atoms of nuclear spin i.

The numerical value of μ_B/h in the frequency scale is 1399.70 kc/s·oersted.

For the ^{39}K resonance ($i = \frac{3}{2}$, $2i+1 = 4$, $g_j = 2$) in an earth field of 0.4 oersted the resonance frequency ν_F is located near 279.940 kc/s.

For ^{39}K the nuclear magnetic moment in units of μ_n is $ig_i' = 0.391$, which corresponds in units of μ_B to $ig_i = 0.391/1839$ and hence the difference

$$\nu_{F_1} - \nu_{F_2} = \frac{\mu_B H}{h} 2g_i = 159 \text{ c/s}$$

in a field of 0.4 gauss.

This turns out to be small compared to the second-order splitting of the Zeeman resonances produced by decoupling of electron and nuclear spin, which splits the Zeeman lines of each hyperfine state into $2F$ components, separated by an interval proportional to the square of the field:

$$\Delta\nu = \tfrac{1}{8}\frac{(g_j(\mu_B H/h))^2}{\Delta E_0/h} = 2\frac{\nu_F^2}{\Delta E_0/h}.$$

Here $\Delta E_0/h$ is the hyperfine interval for zero field in the frequency scale:

For ^{39}K we have $\Delta E_0/h = 461$ Mc/s, and in a field of 0.4 oersted where $\nu_F \sim 280$ kc/s, this interval is

$$\Delta\nu = 2\frac{(280)^2}{461.000} = 340 \text{ c/s}.$$

We observe four components for $F_1 = 2$ (a, b, c, d) and two components for $F_2 = 1$ (e and f), according to Fig. 39.

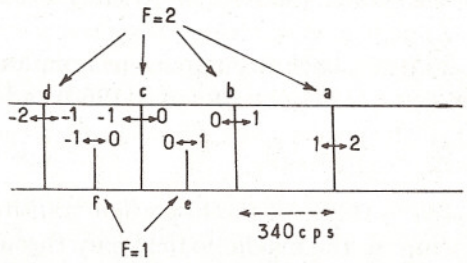

Fig. 39. Hyperfine structure of the Zeeman-resonance line of ^{39}K in the earth magnetic field ($H_0 = 0.4$ gauss).

The relative intensities of these components depend on the pumping conditions, especially on the sign of the circularly polarized pumping-light (σ^+ or σ^-). For σ^+ light the a component ($F = 2$, $m = 2 \to 1$ transition) on the high-frequency side is the strongest and can easily be recognized and separated from the other components.

Putting $x = \mu_B H/h = 1399.70$ kc/s, the frequency of component a is given in kc/s by the formula;

$$\nu_a = \tfrac{1}{2}x\left[1+\frac{3}{2}\cdot\frac{x}{\Delta E_0/h}\right] = \tfrac{1}{2}x\left[1+3.26\times10^{-6}x\right].$$

From the measured frequency ν_a, the numerical values of x and H can be easily deduced.

As the line-width is of the order of 10 c/s and as the center of the line can be easily located with a precision of ± 0.1 c/s, the field value is known with an accuracy of $\pm 10^{-7}$ oersted.

Using a feed-back technique the variation of the field value as a function of time can be recorded. Figure 40 shows an example of such an automatic recording of the earth field in a quiet region located outside an industrial area.

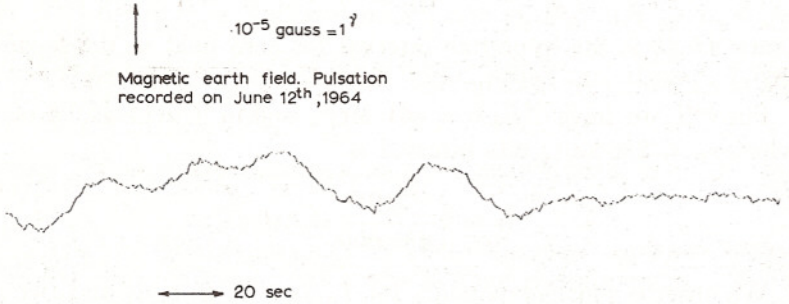

Fig. 40. Automatic recording of the variations of the earth magnetic field with a ^{39}K magnetometer (courtesy of J. Mosnier, Paris, E.N.S.).

Magnetometers using optical-pumping techniques are described by MALNAR and MOSNIER [1961], by BENDER [1960] and by BLOOM [1962].

4.2. FREQUENCY STANDARDS

The $m = 0 \leftrightarrow m = 0$ line of the hyperfine transition $\Delta F = 1$ of an alkali atom depends on the magnetic field only through a second-order term which is very small in weak fields. According to the Breit–Rabi formula the frequency ν of this transition is given by

$$\nu = \nu_0(1+\tfrac{1}{2}z^2)$$

where

$$\nu_0 = \Delta E_0/h$$

and where

$$z = (g_j-g_i)\mu_B H/\Delta E_0 = (g_j-g_i)\mu_B H/h\nu_0.$$

Neglecting g_i against g_j we can write this equation in the form

$$\nu = \nu_0+\tfrac{1}{2}(g_j\mu_B/h)^2\cdot H^2/\nu_0.$$

For ^{133}Cs ($\nu_0 \approx 9193$ Mc/s) and ^{87}Rb ($\nu_0 \approx 6835$ Mc/s) the numerical values are

$$^{133}\text{Cs: } \nu = \nu_0+427 \text{ c/s}\cdot H^2(\text{oersted})$$
$$^{87}\text{Rb: } \nu = \nu_0+574 \text{ c/s}\cdot H^2(\text{oersted}).$$

In a field of $H = 10^{-2}$ oersted, the difference $\nu-\nu_0 \approx 5\times10^{-2}$ c/s and the relative error arising from neglecting this difference is of the order of $(\nu-\nu_0)/\nu_0 = 10^{-11}$.

A field of $H = 10^{-2}$ oersted is sufficient to separate the field-dependent transitions from the 0, 0 transition. The frequencies of the nearest field-dependent transitions ($m = 0 \to m = \pm 1$) are given by

$$\nu = \nu_0 + \frac{g_j}{2i+1}\frac{\mu_B}{h}H.$$

For ^{87}Rb ($i = \frac{3}{2}$) this gives

$$\nu_{\pm1} = \nu_0 \pm 7\times10^5 \text{ c/s}\cdot H(\text{oersted}).$$

In a field of $H = 10^{-2}$ oersted the corresponding frequency interval is $\nu_1-\nu_0 = 7$ kc/s.

As the line-breadth is smaller than 0.1 kc/s the side-lines can be easily separated from the 0, 0 line, and the measurement of their distance to the central 0, 0 line gives the exact value of H and permits the evaluation of the quadratic correction term for the 0, 0 line frequency.

The realization of frequency standards based on the optical-pumping technique has been discussed by ARDITI [1960] who has constructed standards working on the 1772 Mc frequency of ^{23}Na and on the 9193 Mc frequency of ^{133}Cs.

Frequency standards using the 6835 Mc frequency of ^{87}Rb have been constructed on a commercial scale in U.S.A. and in France (C.S.F. [1964]). In the case of ^{87}Rb the technique of hyperfine pumping (§ 2.1.1.3) assures an excellent signal to noise ratio.

Figure 41 shows the block diagram of a rubidium atomic clock. The Rb hyperfine frequency is compared to the frequency of a harmonic

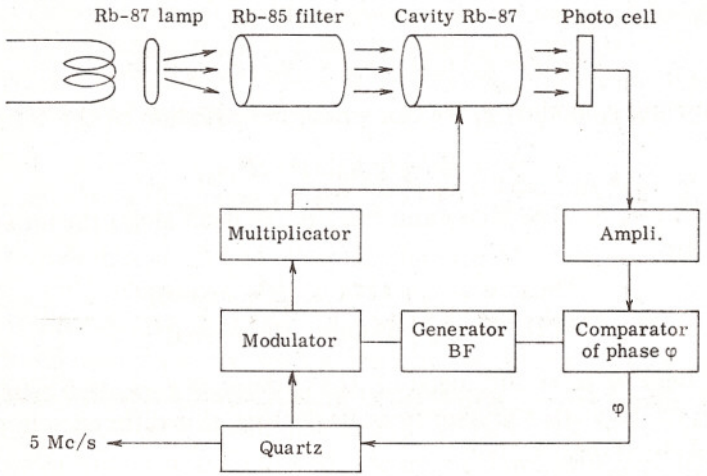

Fig. 41. Block diagram of a ^{87}Rb frequency standard.

of a quartz oscillator whose frequency in the range of 5 Mc/s can be tuned by a condenser circuit.

The frequency of the quartz is multiplied in successive steps to reach a frequency near 6835 Mc/s. The small microwave power delivered by the multiplication chain is directly applied to the rubidium cell and causes the hyperfine transitions which are optically detected. The frequency of the quartz oscillator is modulated by a low-frequency generator while the quartz frequency is scanned slowly through the atomic transition. An 'error signal' of dispersion shape results as is seen in Fig. 42. This error signal is used through a feed-back to maintain the harmonic of the quartz on the center of the hyperfine 0, 0 line. The whole device has to be temperature stabilized. The illumination conditions must be chosen carefully to avoid frequency shifts by light (§ 3.4).

The frequency stability of the model constructed by C.S.F. has been tested by studying the beat frequency of two independent identical clocks. The frequency fluctuations during several hours are of the order of

$$\Delta\nu/\nu = 3\times10^{-11}.$$

Transportable models of small weight have been constructed.

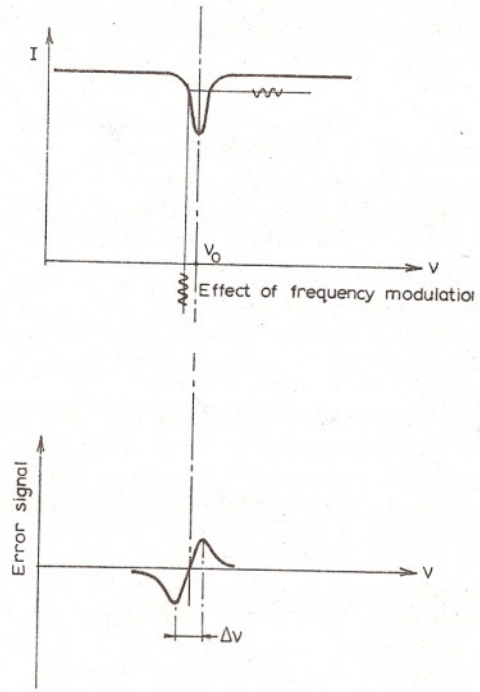

Fig. 42. Low-frequency modulation of the resonance signal results in a dispersion-shaped error curve giving the feed-back signal.

§ 5. Extensions of Optical-Pumping Techniques

Most of the experiments performed with optical-pumping techniques have been made on neutral atoms in dilute gases and vapours. Interesting attempts have been made to extend optical-pumping techniques to the study of ions either in the gas phase or in solids.

We must restrict ourselves to give here the principal references:

Work on ions in the gas phase has been made by DEHMELT and coworkers: DEHMELT and JEFFERTS [1962], JEFFERTS and DEHMELT [1962], DEHMELT and MAJOR [1962], MAJOR and DEHMELT [1962].

The application of optical-pumping techniques to ions in solids has been reviewed by KASTLER [1963b].

Interesting results have been obtained by Margerie and coworkers on Cr^{+++} ions in ruby and on F-centers in alkali halides (BROSSEL and MARGERIE [1963], KARLOV *et al.* [1963] and MARGERIE [1965]).

Finally we may mention that optical-pumping techniques are used

in most of the solid state lasers and in the Cs-vapour laser to obtain population inversion (JACOBS [1961], LENGYEL [1962], BENNETT [1962], HEAVENS [1963, 1964]).

References

ABELLA, I. D., 1962, Phys. Rev. Letters **9**, 453.
ABRAGAM, A., 1961, The Principles of Nuclear Magnetism (Clarendon Press, Oxford).
ADRIAN, F. J., 1960, J. Chem. Phys. **32**, 973.
ADRIAN, F. J., 1962, Phys. Rev. **127**, 837.
ALEKSANDROV, E. B. and V. A. KHODOVOI, 1962, Optics and Spectroscopy **13**, 424.
ALEKSANDROV, E. B., 1963, Opt. i. Spektroskopiya **14**, 436 (American translation, 1963, **14**, 233).
ANDERSON, L. W. and F. M. PIPKIN, 1959, Phys. Rev. **116**, 87.
ANDERSON, L. W., F. M. PIPKIN and J. C. BAIRD, 1960, Phys. Rev. **120**, 1279.
ANDERSON, L. W. and A. T. RAMSEY, 1961, Phys. Rev. **124**, 1862.
ANDERSON, L. W. and A. T. RAMSEY, 1963, Phys. Rev. **132**, 712.
ARDITI, M. and T. R. CARVER, 1958a, Phys. Rev. **109**, 1012.
ARDITI, M. and T. R. CARVER, 1958b, Phys. Rev. **112**, 449.
ARDITI, M., 1960, Annales de Physique **5**, 973.
ARDITI, M. and T. R. CARVER, 1961, Phys. Rev. **124**, 800.
ARDITI, M. and T. R. CARVER, 1965, J. Appl. Phys. **36**, 443.
BALLING, L. C., R. J. HANSON and F. M. PIPKIN, 1964, Phys. Rev. **133A**, 607.
BARRAT, J. P., 1959, Thesis Paris; and J. de Phys. **20**, 541, 633, 657.
BARRAT, J. P. and C. COHEN-TANNOUDJI, 1961, C. R. Ac. Sci. **252**, 93 and 255; J. de Physique **22**, 329 and 443.
BARRAT, J. P., 1961, Proc. Roy. Soc. A**263**, 371.
BEATY, E. C., P. L. BENDER and A. R. CHI, 1958, Phys. Rev. **112**, 450.
BELL, W. E. and A. L. BLOOM, 1957, Phys. Rev. **107**, 1559.
BELL, W. E. and A. L. BLOOM, 1958, Phys. Rev. **109**, 219.
BELL, W. E. and A. L. BLOOM, 1961, Phys. Rev. Letters **6**, 280.
BENDER, P., 1956, Thesis Princeton University.
BENDER, P. L., E. C. BEATY and A. R. CHI, 1958, Phys. Rev. Letters **1**, 311.
BENDER, P. L., 1960, Comptes-Rendus 9e Colloque Ampère, Pisa, p. 621.
BENNETT, W. R., 1962, Applied Optics, Supplement on Optical Masers (Methuen, London) p. 24.
BENUMOF, R., 1965, Am. J. of Physics **33**, 151.
BERNHEIM, R. A., 1962, J. Chem. Phys. **36**, 135.
BESSET, C., J. HOROWITZ, A. MESSIAH and J. WINTER, 1954, J. de Physique **15**, 251.
BITTER, F., 1962, Applied Optics **1**, 1.
BLOCH, F., 1946, Phys. Rev. **70**, 460.
BLOOM, A. L. and J. B. CARR, 1960a, Phys. Rev. **119**, 1946.
BLOOM, A. L., 1960b, Scientific American **203**, 72.
BLOOM, A. L., 1962, Applied Optics **1**, 61.
BOUCHIAT, M. A., 1962, C. R. Ac. Sci. **254**, 3650 and 3828.
BOUCHIAT, M. A., 1963, J. de Physique **34**, 379 and 611.

BOUCHIAT, M. A. and J. BROSSEL 1963, C. R. Ac. Sci. **257**, 2825.
BOUCHIAT, M. A., 1964, Thesis Paris, to be published.
BREWER, R., 1962, J. Chem. Phys. **37**, 2504.
BREWER, R., 1964, J. Chem. Phys. **40**, 1077.
BROSSEL, J., 1952, Annales de Physique **7**, 622
BROSSEL, J. and F. BITTER, 1952, Phys. Rev **86**, 308.
BROSSEL, J., B. CAGNAC and A. KASTLER, 1953, C. R. Ac. Sci. **237**, 984.
BROSSEL, J., B. CAGNAC and A. KASTLER 1954, J. de Physique **15**, 6.
BROSSEL, J., 1957, La Spectroscopie des Radiofréquences (Edition Revue d'Optique, Paris) p. 65,
BROSSEL, J., 1960a, Year Book Phys. Soc. (London) p. 1.
BROSSEL, J., 1960b, Renpiconti S.I.F., XVII Corso (Academic Press, New York) p. 187.
BROSSEL, J., 1960c, Quantum Electronics, vol. 1 (Columbia Un. Press) p. 81.
BROSSEL. J., 1961, Quantum Electronics, vol. 2 (Columbia Un. Press) p. 95.
BROSSEL, J. and J. MARGERIE, 1963. In: Low, W., ed., Paramagnetic Resonance, vol. 2 (Academic Press, New York) p. 535.
CAGNAC, B., 1960, Annales de Physique **6**, 467.
CARVER, T. R., 1959, The Ann Arbor Conference on Optical Pumping (Edited by the University of Ann Arbor, Michigan) p. 29.
CARVER, T. R., 1963, Science **141**, 599.
CLARKE, Y. A., 1962, J. Chem. Phys. **36**, 2211.
COHEN-TANNOUDJI, C., J. BROSSEL and A. KASTLER, 1957, C. R. Ac. Sci. **245**, 1027.
COHEN-TANNOUDJI, C., 1961a, Advances in Quantum Electronics (Columbia Un. Press) p. 114.
COHEN-TANNOUDJI, C., 1961b, C. R. Ac. Sci. **252**, 394.
COHEN-TANNOUDJI, C., 1961c, C. R. Ac. Sci. **253**, 2662.
COHEN-TANNOUDJI, C., 1961d, C. R. Ac. Sci. **253**, 2899.
COHEN-TANNOUDJI, C., 1962a, Annales de Physique **7**, 423 and 469; Thesis Paris, 1962.
COHEN-TANNOUDJI, C., 1962b, Rendiconti S.I.F., XVII Corso (Academic Press, New York) p. 240.
COHEN-TANNOUDJI, C., 1963, J. de Physique **24**, 653.
COLEGROVE, F. D., P. A. FRANKEN, R. R. LEVIS and R. H. SANDS, 1959, Phys. Rev. Letters **3**, 420.
COLEGROVE, F. D., L. D. SCHEARER and G. K. WALTERS, 1963, Phys. Rev. **132**, 2561.
C.S.F., 1964, Compagnie Générale de Télégraphie sans Fil, 7c (Bd. Haussmann, Paris, 8e) Notice no. 1602.
DAVIDOVITS, P. and W. A. STERN, 1965, Appl. Phys. Letters **6**, 20.
DEHMELT, H. G., 1957a, Phys. Rev. **105**, 1487.
DEHMELT, H. G., 1957b, Phys. Rev. **105**, 1924.
DEHMELT, H. G., 1958, Phys. Rev. **109**, 381.
DEHMELT, H. G. and K. B. JEFFERTS, 1962, Phys. Rev. **125**, 1318.
DEHMELT, H. G. and F. G. MAJOR, 1962, Phys. Rev. Letters **8**, 213.
DICKE, R. H., 1953, Phys. Rev. **89**, 472.
DODD, J., W. FOX, G. W. SERIES and M. TAYLOR, 1959, Proc. Phys. Soc. **74**, 789.
FRANKEN, P., R. SANDS and J. HOBART, 1958, Phys. Rev. Letters **1**, 118.
FRANKEN, P., 1961, Phys. Rev. **121**, 508.

FRANZEN, W., 1959, Phys. Rev. ***115***, 850.
FRED, M., S. F. TOMKINS, J. K. BRODY and M. HAMERMESH, 1951, Phys. Rev. ***82***, 406.
GLASSGOLD, A. E., 1963, Phys. Rev. ***132***, 2144.
GOZZINI, A., 1962, C. R. Ac. Sc. ***255***, 1905.
GROSSETÊTE, F., 1964a, J. de Physique ***25***, 388.
GROSSETÊTE, F., 1964b, C. R. Ac. Sci. ***258***, 3668.
GUIOCHON, M. A., J. E. BLAMONT and J. BROSSEL, 1957, J. de Physique ***18***, 99.
HACK, M. N., 1956, Phys. Rev. ***104***, 84.
HARTMANN, F., M. RAMBOSSON, J. BROSSEL and A. KASTLER, 1958, C. R. Ac. Sci. ***246***, 1522.
HEAVENS, O. S., 1962, Applied Optics, Supplement on Optical Masers (Methuen, London).
HEAVENS, O. S., 1964, Optical Masers (Methuen, London).
HERMAN, R. M., 1964, Publication of the TRW Space Technology Laboratories, California.
HOBART, J. L., 1962, Thesis Michigan University.
HOLLOWAY, W. W., E. LUSCHER and R. NOVICK, 1962, Phys. Rev. ***126***, 2109.
JACOBS, S., G. GOULD and P. RABINOWITZ, 1961, Phys. Rev. Letters ***7***, 451.
JARRETT, S. M., 1962, Thesis Michigan University.
JEFFERTS, K. B. and H. G. DEHMELT, 1962, Bull. Am. Phys. Soc. ***7***, 432.
KARLOV, N. V., J. MARGERIE and MERLE D'AUBIGNÉ, 1963, J. de Physique ***24***, 717.
KASTLER, A., 1950, J. de Physique ***11***, 255.
KASTLER, A., 1954, Proc. Phys. Soc. A***67***, 853.
KASTLER, A., 1957a, J. Opt. Soc. Am. ***47***, 460.
KASTLER, A., 1957b, Nuovo Cimento Série X, vol. 6, suppl. No. 3, 1148.
KASTLER, A., 1960, Rendiconti Scuola Internat. Fisica, XVII Corso (Academic Press, New York) p. 157.
KASTLER, A., 1961, C. R. Ac. Sci. ***252***, 2396.
KASTLER, A., 1962, Proc. XIth Colloque Ampère Eindhoven (North-Holland Publ. Co., Amsterdam) p. 14.
KASTLER, A., 1963a, J. Opt. Soc. Am. ***53***, 902.
KASTLER, A., 1963b. In: Chang, W. S. C. ed., Lasers and Applications (Ohio State University, Columbus).
KLEPPNER, D., H. M. GOLDENBERG and N. F. RAMSEY, 1962, Phys. Rev. ***126***, 603.
LAMB, W. E., 1951, Proc. Phys. Soc. A ***14***, 19.
LAMBERT, R. H. and F. M. PIPKIN, 1962, Phys. Rev. ***128***, 198.
LAMBERT, R. H. and F. M. PIPKIN, 1963, Phys. Rev. ***129***, 1233.
LEHMANN, J. C. and R. BARBÉ, 1963, C. R. Ac. Sci. ***257***, 3152.
LEHMANN, J. C. and J. BROSSEL, 1964, C. R. Ac. Sci. ***258***, 869.
LEHMANN, J. C. and C. COHEN-TANNOUDJI, 1964a, C. R. Ac. Sci. ***258***, 4463.
LEHMANN, J. C., 1964b, J. de Physique, ***25***, 809.
LENGYEL, B. A., 1962, LASERS (J. Wiley and Sons, New York).
MCNEAL, R. J., 1964, J. Chem. Phys. ***40***, 1089.
MAJOR, F. G. and H. G. DEHMELT, 1962, Bull. Am. Phys. Soc. ***7***, 432.
MALNAR, L. and J. P. MOSNIER, 1961, Annales de Radioélectricité ***16***, no. 63.

MANUEL, J. and C. COHEN-TANNOUDJI, 1963, C. R. Ac. Sci. ***257***, 413.
MARGENAU, H., P. FONTANA and L. KLEIN, 1959, Phys. Rev. ***115***, 87.
MARGERIE, J., 1955, C. R. Ac. Sci. ***241***, 865.
MARGERIE, J. and J. BROSSEL, 1955, C. R. Ac. Sci. ***241***, 373.
MARGERIE, J., J. BROSSEL and J. M. WINTER, 1955, C. R. Ac. Sci. ***241***, 566.
MARGERIE, J., 1965, Thesis Paris.
MITCHELL, A. C. G. and M. W. ZEMANSKY, 1934, Resonance Radiation and Excited Atoms (Cambridge Un. Press).
NEDELEC, O., M. N. DESCHIZEAUX and J. C. PEBAY-PEYROULA, 1963, C. R. Ac. Sci. ***257***, 3130.
NOVICK, R. and H. E. PETERS, 1958, Phys. Rev. Letters ***1***, 120.
OMONT, A. and J. BROSSEL, 1961, C. R. Ac. Sc. ***252***, 710.
PIPKIN, F. M. and R. H. LAMBERT, 1962, Phys. Rev. ***127***, 787.
POPESCU, I. M. and L. N. NOVIKOV, 1964, C. R. Ac. Sci. ***259***, 1321.
ROBINSON, H. G., E. S. ENSBERG and H. G. DEHMELT, 1958, Bull. Am. Phys. Soc. ***3***, 9.
ROBINSON, K. B., 1960, Phys. Rev. ***117***, 1275.
RUBINOWICZ, A., 1918, Physikalische Zeitschrift ***19***, 441 and 465.
SALWEN, H., 1955, Phys. Rev. ***99***, 1274.
SALWEN, H., 1956, Phys. Rev. ***101***, 623.
SERIES, G. W., 1959, Reports on Progress in Physics ***22***, 280.
SHEARER, L. D., 1962, Phys. Rev. ***127***, 512.
SIBILLA, J. T., 1962, Thesis Princeton University.
SKALINSKI, T., 1960, Rendiconti della S.I.F., XVII Corso (Academic Press, New York, 1962) p. 212.
SKROTSKY, G. V. and T. G. IZIOUMOVA, 1961, Soviet Physics Uspekhi ***4***, 177.
STAVN, M. J., 1963, Thesis M.I.T.; and 1964, Bull. A.P.S. ***9***, 10.
TORREY, H. C., 1949, Phys. Rev. ***76***, 1059.
WALTER, W. T., 1962, Thesis M.I.T.; and Bull. A.P.S. ***7***, 295.
WINTER, J. M., 1955a, C. R. Ac. Sci. ***241***, 375.
WINTER, J. M., 1955b, C. R. Ac. Sci. ***241***, 600.
WINTER, J. M., 1959, Annales de Physique ***4***, 745.
WINTER, J. M., 1962, Rendiconti S.I.F., XVII Corso (Academic Press, New York) p. 259.
WITTKE, J. P. and R. H. DICKE, 1954, Phys. Rev. ***96***, 340.
ZAFRA, R. DE, 1960, American Journal of Physics ***28***, 646.